



# Comparison of electrocoagulation and combined electrocoagulation-electrooxidation treatment for synthetic tannery wastewaters bearing phenolic syntan

Amit Kumar · D. Basu

Received: 11 April 2023 / Accepted: 26 March 2024 / Published online: 13 April 2024  
© The Author(s), under exclusive licence to Springer Nature Switzerland AG 2024

**Abstract** In this study, EC process using an aluminum anode, and EC-EO process using aluminum and mixed metal oxide, i.e., platinum-ruthenium dioxide-coated onto titanium (Al-Ti/Pt-RuO<sub>2</sub>) anode was used to understand the remove of phenolic syntan (PS) from synthetic tannery wastewaters. The operational conditions of the abovementioned electrochemical processes were optimized using Taguchi L<sub>16</sub> method in terms of maximum removal of total organic carbon (TOC) and PS. At the optimum operating condition (current density = 14.25 mA/cm<sup>2</sup>, initial pH = 4, rotational speed = 70 rpm and initial PS amount = 0.25 g/L), the incomplete removal of TOC (83.93%) and PS (81.19%) was obtained in the EC process with the energy consumption of 0.135 kWh/g TOC remove and 0.056 kWh/g PS remove. In contrast, almost (≈100%) complete removal of the dissolved organic pollutant was observed in the EC-EO process with the energy consumption of 0.113 kWh/g TOC remove and 0.0453 kWh/g PS remove. The energy consumption per g TOC and PS removed was 0.135 and 0.056 kWh for the EC process, whereas 0.113 and 0.0453 kWh for the EC-EO process. The operating cost of the EC-EO process was estimated

to be 1.39 USD/m<sup>3</sup>, which was lesser (-19.65%) than the operating cost of the EC process. Signal-to-noise ratio and ANOVA results showed that current density was the most influential parameter with the highest delta value and contribution ratio for TOC and PS removal in both the EC and EC-EO process. The UV/Vis and FT-IR analyses indicate that the highest removal of aromatic compounds was obtained in the EC-EO process compared to the EC process. FT-IR analyses confirmed that the PS was first degraded into a quinone functional group, which was further oxidized into carboxylic acid.

**Keywords** Combine EC-EO process · Rotating electrode · Phenolic syntan · Taguchi method

## 1 Introduction

Leather production is a significant economic sector in several developing and developed nations. The tanning process transforms putrefying skins and hides into non-putrefying leather through chemical operations, the most essential step in the entire leather-making process (Ozgunay et al., 2007). Tanning practice produces 30–40 m<sup>3</sup> of wastewater in addition to solid wastes containing heavy metals, aromatic organic and inorganic compounds, per tonne of hide/skin (Song et al., 2003; Tripathi et al., 2011). Phenolic syntans (PS) are artificial tanning chemicals utilized in pre-tanning and re-tanning operations to transform skins

A. Kumar (✉) · D. Basu  
Motilal Nehru National Institute of Technology Allahabad,  
Prayagraj 211004, India  
e-mail: amitkumar@mnnit.ac.in

D. Basu  
e-mail: basud@mnnit.ac.in

into imputrescible leather. PS are produced by polymerizing high molecular weight organic substances such as phenols with formaldehyde and sulfonic acid (Rema et al., 2010). The wastewater from the tannery contains just 50% of the syntans that are not absorbed by the skin. The phenol and phenolic compounds are dangerous to humans, aquatic life, and the environment (Michalowicz & Duda, 2007). Phenolic syntan also indicated that *Daphnia magna* was substantially immobilized by a syntan concentration of 100–300 mg/L (Lofrano et al., 2007).  $EC_{50}$  values for *Daphnia magna* were set at 364 mg/L for synthetic tannin (poly-condensed phenols with formaldehyde) at 24 h exposure time (Lofrano et al., 2008). As a result, these syntans might linger in water for a long time, having direct ecotoxicological consequences on aquatic life (Rivera-Utrilla et al., 2002; De Nicola et al., 2007). Biologically, these substances are hard to degrade because they have an aromatic ring with a sulfonic group that resists bacterial attack (Virginija et al., 2014).

Several practices such as adsorption (Li et al., 2013), coagulation–flocculation (Ginos et al., 2006), biological treatment (Tisler & Koncan, 1997; Danhong et al., 2008; Ganesh & Ramanujam, 2009), photocatalytic degradation (Sundarapandiyam et al., 2017), ozonation (Thankappan et al., 2017) have been suggested in the literature for the removal of syntan from tannery wastewaters. Adsorption and coagulation–flocculation processes were reported to have drawbacks such as frequent absorbent regeneration and significant sludge production (Can et al., 2006). The biodegradation of phenolic syntan was found to be difficult due to its toxicity to common remediating microorganisms (Tisler & Koncan, 1997; Danhong et al., 2008; Ganesh & Ramanujam, 2009). Although ozonation and photochemical degradation are effective, they have significant operational costs (Can et al., 2006; Ferella et al., 2013). Most tanneries in developing nations are small-scale and cannot afford to build and maintain expensive treatment facilities because effluent treatment plants (ETPs) are prohibitively expensive to build and operate. They also generate a considerable amount of sludge. As a result, alternative treatment techniques must be evaluated and suggested as in-house treatment options for tanneries.

The electrochemical method is effective for the removal of organic compounds from wastewater. This technique has been widely investigated for the

treatment of numerous industrial pollutants discharged by tanneries (Min et al., 2004; Sundarapandiyam et al., 2010), textile industries (Raju et al., 2008), olive oil mills (Tavares et al., 2012), and other organic compounds including nonyl phenol ethoxylates (Ciorba et al., 2002), benzoquinone (Yoon et al., 2007), and chlorophenols (Cañizares et al., 2004). Recently, several studies have been conducted for treating phenol-based wastewater using electrochemical techniques (Panizza, 2000; Li et al., 2009; Belaid et al., 2013; Olya & Pirkarami, 2013). Electrochemical technologies, including electrocoagulation (EC) and electro-oxidation (EO), are receiving considerable attention due to their capacity to treat wastewater adequately. EC is an effective approach for the treatment of water and wastewater that depends on the electrochemical disintegration of sacrificial electrodes (aluminum) into metal cations (Kumar & Basu, 2022a, b). These metal cations are then transformed into metal hydroxide flocs, which promote the coagulation, adsorption, and precipitation of suspended and colloidal pollutants. EC is distinct from traditional chemical coagulation as the coagulant is generated in-situ, without the need for adding chemicals from external source. A reduced quantity of sludge production is one of the main advantages of the EC procedure. This leads to reducing the possibility of secondary pollution and sludge treatment costs (Kumar & Basu, 2022a, b). Additional benefits of the EC method include its simple design, ease of operation, lesser electrolysis duration, and lower maintenance, making it a convenient treatment process (Kumar & Basu, 2022a, b; Gurses et al., 2022). Very few studies have been reported in literature related to the elimination of tanning agents from effluents by the EC process. Hassoune et al., (2017) studied the applicability of EC techniques in the removal of aqueous tannins from tannery wastewater. The authors have reported on the use of Al electrodes in the removal of chestnut (97.4%) and mimosa (97.7%) tannins at the optimum CD of 47.6 A/m<sup>2</sup> and 71.4 A/m<sup>2</sup>, respectively. Murugananthan et al., (2005) obtained higher COD removal (99.5%) within a pH range of 8.0–9.0 for Syntan Relugan RR with Al electrodes based EC process at the operating CD value of 47 mA/cm<sup>2</sup>, and treatment duration of 15 min.

EO has emerged as an effective method for eliminating persistent or refractory organic compounds from industrial effluents (Sarkka et al., 2015; Zhu

et al., 2010). Application of the EO technique for treatment of industrial pollutants has three main benefits: (1) the removal of redox substances, which avoids the necessity to treat wasted redox streams; (2) precise control of specific reactions through adjusting applied voltage or current; (3) enhanced capabilities of the onsite treatment technique (Panizza & Cerisola, 2005). There are two ways to oxidize organic matter: (i) directly (on anode surfaces), which produces water and  $\text{CO}_2$  primarily, and, (ii) indirectly, when effective oxidants formed electrochemically, such as ozone, hypochlorite, and chlorine, are present). It could result in the total mineralization of the organic substances into carbon dioxide, water and/or other inorganic substances (Moreira et al., 2017; Radjenovic & Sedlak, 2015). Some studies have been performed on removing tanning agent sytan from wastewater through the EO process. Vijayalakshmi et al., (2011) studied the treatment of tannery wastewater by EO process using mixed metal oxide (MMO) electrode made by titanium mesh coated with  $\text{IrO}_2$ ,  $\text{TaO}_2$ , and  $\text{TiO}_2$ . The authors reported that the TOC reduction was hardly 50% at the CD  $37.03 \text{ mA/cm}^2$  after 6 h of electrolysis time. Vocciante et al., (2021) reported on the removal of synthetic tannins by the EO technique with Ti/Pt and Ti/ $\text{PbO}_2$  electrodes, showing that the Ti/ $\text{PbO}_2$  electrode eliminated 100% of COD under the operating conditions of CD:  $300 \text{ A/m}^2$ ; initial synthetic tannin concentration:  $1.5 \text{ g/L}$ ; electrolyte:  $1 \text{ M H}_2\text{SO}_4$ ; electrolysis time: 24 h. Buso et al., (2000) stated that more than 90% removal of COD and no appreciable UV–Vis absorption at 280 nm was observed after 45 min of electrolysis time using platinum electrodes.

Electrochemical processes can be complex treatment methods, due to the influence exerted by various operating factors, as well as the pollutant removal mechanism which is influenced by the individual characteristics of aqueous organic constituents present in the wastewater. Modelling the pollutant removal process by conventional mathematical models is time-consuming and expensive because a large number of experiments need to be conducted to fulfil the requirement of requisite data. When dealing with highly complicated systems, the design of experiments (DOE) method has drawn attention for the prediction and optimization of treatment processes. Genichi Taguchi invented the Taguchi technique (Balki et al., 2016), a statistical approach adopted to

enhance the DOE. The Taguchi technique is systematic, requiring fewer trials and less time, money, and effort, while providing more quantitative data (Stone & Veevers, 1994). It optimizes the operating conditions using a specially constructed orthogonal array (OA) comprised of controllable factors and their variable levels (Taguchi, 1990). The key benefit of Taguchi approach is that it reduces experiment expenses while eliminating variations in product response by setting the mean response on target.

Pollutant removal by EC process can take longer electrolysis time and lead to incomplete treatments in case of high strength industrial effluents containing very high concentrations of colloidal particles and dissolved organics. Conversely, EO can eliminate any remaining soluble contaminants (Linares-Hernandez et al., 2010). It is worth noting that EO requires more energy than EC. Thus, combining these treatment approaches can improve their efficiency while lowering operational expenses. Several other experimental studies have been conducted on the combined EC-EO process using composite electrodes to treat domestic wastewater treatment (Ozyonar & Korkmaz, 2022), ammonia and phosphate (Sun et al., 2020) and restaurant wastewater (Daghrir et al., 2012). These studies showed that the combined EO-EC process using composite/hybrid electrodes was a promising approach to enhance pollutant removal efficiency at relatively lower cost of treatment. However, to the best of knowledge of the authors, the present study is the first of its kind to conduct a comparative study on the removal of aqueous phenolic sytan by the EC and combined EC-EO process using rotating aluminium and composite ( $\text{Al-Ti/Pt-RuO}_2$ ) electrodes. The choice of aluminium and MMO anode was meant to provide in-depth insight into understanding the effect of electrode material on the energy consumption and operating costs of the EC and combined EC-EO processes. The demerits of the individual EC and EO process were expected to be overcome by combining both the processes in the same reactor. Additionally, the study aimed to apply the Design of Experiments (DOE) technique for estimating the best operating conditions for both the electrochemical processes namely EC and combined EC-EO process for treating synthetic tannery wastewaters bearing aqueous phenolic sytan. The electrochemical process can be quite

complex and is influenced by a number of factors such as operating condition, wastewater characteristics, etc. Hence, the performance of the electrochemical unit can be improved by conducting the experiments at optimized operating conditions. The Taguchi technique was adopted to study the relationship between multiple input variables and key output variables (i.e., removal efficiency), so as to select the best possible electrochemical treatment option with the most suitable anode material.

The present work focuses on evaluating the performance of two electrochemical processes, namely the combined EC-EO and EC process in the removal of the targeted contaminants (TOC and phenolic syntan) from synthetic tannery wastewaters. The impact of operating factors, including current density (CD), the rotational speed of the electrode (RSE), initial pH ( $\text{pH}_i$ ) and the initial amount of PS ( $\text{PS}_i$ ) on the removal of targeted pollutants was investigated. The two approaches have been compared in terms of removal efficiency, operating costs and power consumption. The Taguchi ( $L_{16}$ ) method was used to find the optimum operational condition of EC and the combined EC-EO process to remove targeted pollutants. An analysis of variance (ANOVA) was used to examine the contribution of each factor and their interacting impacts, ultimately leading to the selection of the best operating factors. The change in the functional group of phenolic syntan during the treatment was investigated by the FT-IR technique.

## 2 Materials and Procedures

### 2.1 Chemicals used

The commercially available phenolic syntan was purchased from M/s BASF India Ltd., Kanpur, India. Other chemicals were used in the experimental analysis: sodium chloride (AG, 99%, Merck Life Science Pvt. Ltd., Mumbai, India), hydrochloric acid (35.8–36.5%, MOLYCHEM, Mumbai, India), sodium hydroxide pellets (AG, 98%, SRL Pvt. Ltd., Maharashtra, India) and sulfuric acid (AG, 97%, Rankmem, Avantor Performance Materials India Ltd., Thane, Maharashtra, India).

### 2.2 Electrochemical setup and procedure

In this study, the lab-scale electrochemical reactor is shown in Fig. 1. The Plexiglas reactor had a working capacity of 3.0 L. Aluminum was selected as the electrode material in the EC process. During the EC-EO process, a composite anode and Al cathode were employed. The composite MMO anode was made of aluminum and Ti/Pt-RuO<sub>2</sub> (titanium plate coated with platinum and ruthenium oxide). The total surface area of the composite anode is 50% aluminum and 50% Ti/Pt-RuO<sub>2</sub>. Thus, the EC-EO unit was designed to initiate chemical reactions for promoting both coagulation and oxidation. A perforated cylindrical anode and cathode rod were fitted in a mono-polar configuration. The anode and cathode had an overall effective surface area of 210.5 cm<sup>2</sup>. To enhance mixing and prevent contaminant short-circuiting, the anode was kept porous. For every experimental run, the electrode spacing was maintained at 2 cm. A DC power source (0–30 V, 0–5A) is used to provide a regulated electric current to the electrochemical reactor. Table 1 shows the primary reactions that are observed on the anode and cathode in the EC and EC-EO processes (Daneshvar et al., 2006; Hine, 1985; Kobya et al., 2003; Rajkumar et al., 2007).

Electrochemical experimental runs were performed at  $25 \pm 2$  °C in batch mode with 3 L of simulated phenolic syntan (SPS) solutions prepared by dissolving an appropriate amount of phenolic syntan in 1000 ml of di-ionized water. To ensure the effluents had the

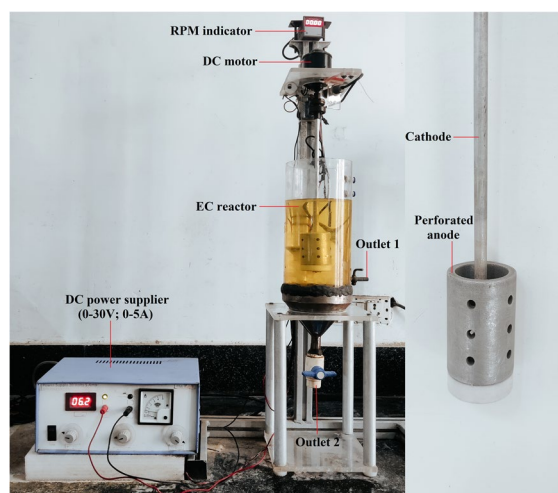


**Fig. 1** Picture of lab scale EC reactor (Kumar & Basu, 2023)

**Table 1** Electrode reactions during the EC and EC-EO processes

|                  | EC process   | EC-EO process  |
|------------------|--|--|
| At anode         | $\text{Al}_{(\text{solid})} \rightleftharpoons \text{Al}^{3+} + 3\text{e}^{-}$ (1)                                   | $2\text{Cl}^{-} \rightarrow \text{Cl}_2 + 2\text{e}^{-}$ (4)<br>$\text{Al}_{(\text{solid})} \rightleftharpoons \text{Al}^{3+} + 3\text{e}^{-}$ (5)   |
| At cathode       | $2\text{H}_2\text{O} + 2\text{e}^{-} \rightleftharpoons \text{H}_{2(\text{gas})} + 2\text{OH}^{-}$ (2)               | $2\text{H}_2\text{O} + 2\text{e}^{-} \rightleftharpoons \text{H}_{2(\text{gas})} + 2\text{OH}^{-}$ (6)   |
| In bulk solution | $\text{Al}^{3+} + 3\text{H}_2\text{O} \rightleftharpoons \text{Al}(\text{OH})_{3(\text{solid})} + 3\text{H}^{+}$ (3) | $\text{Cl}_2 + \text{H}_2\text{O} \rightarrow \text{HClO} + \text{H}^{+} + \text{Cl}^{-}$ (7)<br>$\text{HClO} \rightarrow \text{ClO}^{-} + \text{H}^{+}$ (8)<br>$\text{Al}^{3+} + 3\text{H}_2\text{O} \rightleftharpoons \text{Al}(\text{OH})_{3(\text{solid})} + 3\text{H}^{+}$ (9) |

bare minimum conductivity required for the flow of electric current. Conductivity was kept at 2000  $\mu\text{S}/\text{cm}$  by adding the necessary amount of sodium chloride (NaCl) to the wastewater. It was anticipated that the addition of a strong electrolyte like NaCl would lessen the possibility of electrode passivation which is caused due to the forming an oxide film on the anode surface. Table 2 displays the properties of the SPS solution. The vertically rotatable electrode stirred the reactor's solution. Prior to starting the experiments, 1/10N NaOH and 1/10N HCl solutions were used to adjust the influent pH of the SPS solution. Whatman filter paper with a 0.45  $\mu\text{m}$  pore size was used to filter the samples of treated wastewater. The electrodes were rinsed with 1 M HCl and cleansed with deionized water before the experiment began to remove contaminants from their surface.

### 2.3 Analytical Method

The degradation of phenolic syntan was evaluated by a UV/Vis spectrophotometer (LABINDIA UV-300) at 280 nm. This research confirmed the existence of aromatic structured organic substances in SPS solution by spectral analysis at a wavelength of UV<sub>280</sub> nm. The TOC of the treated and untreated samples was measured by a TOC analyzer (TOC-L, SHIMADZU).

The conductivity and pH of the solution were measured using a calibrated conductivity meter (Lutron CD-4302) and an automatic digital pH meter (HANNA HI 2210). Fourier transform infrared (FT-IR) analysis of the treated and untreated samples has been carried out in order to understand the changes in functional groups within phenolic syntan. The Fourier transform infrared (FT-IR) spectra were obtained between the wave numbers of 4000 to 450  $\text{cm}^{-1}$  using FT-IR spectroscopy (JASCO-V600, SCHIMADZU).

The energy consumption per gram of pollutant removal (EEC) was calculated as per Garg and Prasad, (2015).

The price of materials (primarily electrodes), electric energy, and chemicals utilized in the treatment process are considered in the calculation of the operating cost (OC) of the EC process. The OC has been determined as per Eq. (10) outlined by Kumar and Basu, (2022a, b).

$$\text{OC} \left( \frac{\text{USD}}{\text{m}^3} \right) = (\text{A} \times \text{ELC}) + (\text{B} \times \text{chemical used}) + (\text{C} \times \text{E}) \quad (10)$$

where A, B and are the prices of electrode material, chemicals and electric energy, respectively, in USD.

Kumar and Basu, (2022a, b) suggested the expression of electrode consumption (ELC).

**Table 2** Characteristics of synthetic wastewater

| Characteristics                          | Value                                   |  |  |  |
|--|---|--|--|--|
|  | Dissolve 0.25 g of PS in 1.0 L of water | Dissolve 0.5 g of PS in 1.0 L of water | Dissolve 1.0 g of PS in 1.0 L of water | Dissolve 1.5 g of PS in 1.0 L of water |
| pH                                       | 6.7–7.2                                 | 6.7–7.2                                | 6.7–7.2                                | 6.7–7.2                                |
| TOC (mg/l)                               | 100 ± 5                                 | 200 ± 6                                | 400 ± 5                                | 600 ± 4                                |
| UV <sub>280</sub> absorbance             | 1.325                                   | 2.65                                   | 5.3                                    | 7.95                                   |
| Conductivity ( $\mu\text{S}/\text{cm}$ ) | 750 ± 50                                | 750 ± 50                               | 750 ± 50                               | 750 ± 50                               |

$$ELC\left(\frac{KgAl}{m^3}\right) = \frac{(M \times I \times t)}{(n \times F \times v)} \tag{11}$$

Here, “M” is the molar mass of aluminum (27 g/mol), “n” is the number of electron transfers (n=3 for Al), “t” is the EC time (sec), “F” is the Faraday constant (96,485 C/mol) and “v” is the volume (m<sup>3</sup>). Energy consumption per unit volume treated (E) was determined from Eq. (12) (Kumar & Basu, 2022a, b).

$$E\left(\frac{kWh}{m^3}\right) = \frac{V \times I \times t}{q \times 1000} \tag{12}$$

where “V” is the potential in volts, “I” is current in amp, “t” is the electrolysis period in min, and “q” is the volume of the treated wastewater in m<sup>3</sup>.

The current efficiency (CE) value was computed by dividing the experimental value of electrode consumption by the theoretical value of electrode consumption (AlJaberi, 2019).

AlJaberi, (2019) provided the following expression of Ohmic potential drop:

$$Ohmic\ potential\ drop = \frac{CD * S}{K} \tag{13}$$

where S=spacing between the anode and cathode, CD=current density (mA/cm<sup>2</sup>), and K=conductivity of the solution.

### 2.4 Taguchi optimization study

In this work, all of the variables impacting the performance of the electrochemical process were optimized using Taguchi’s design of experiment (DOE) approach. The variables used for this study are CD, pH<sub>i</sub>, RSE, and PS<sub>i</sub>. Table 3 summarizes the

**Table 3** Variables and their levels

| Variables | Factor                   | Levels |      |     |       |
|-----------|--------------------------|--------|------|-----|-------|
|           |                          | 1      | 2    | 3   | 4     |
| A         | CD (mA/cm <sup>2</sup> ) | 2.375  | 4.75 | 9.5 | 14.25 |
| B         | pH <sub>i</sub>          | 3      | 4    | 5   | 6     |
| C         | RSE (rpm)                | 0      | 40   | 70  | 100   |
| D         | PS <sub>i</sub> (g/L)    | 0.25   | 0.5  | 1   | 1.5   |

variables and their ranges. For statistical analysis, the electrolysis time was fixed as 50 min.

Taguchi’s L<sub>16</sub> orthogonal array (OA) was employed to determine the optimum operating conditions for maximum PS and TOC removal in an electrochemical process. Even the conventional full factorial approach requires significantly more experimental trials (4<sup>4</sup>=256 runs) to attain the optimal conditions. The Taguchi approach uses a novel OA design to plan and evaluate the optimal working conditions with a small number of trials (Zolgharnein et al., 2013, 2014). The number of experimental runs (N) in the Taguchi design is determined by the number of selected parameters (P) and their levels (L) using Eq. (14) (Dhawane et al., 2016):

$$N = (L - 1)P + 1 \tag{14}$$

Table 4 shows the L<sub>16</sub> OA experimental design used in the present study, which needed just sixteen experimental runs.

The optimization criteria were chosen based on the performance characteristics, i.e., the signal-to-noise (S/N) ratio. Performance characteristics are classified into three types: larger is better, smaller is better and nominal is better. The performance

**Table 4** Taguchi L<sub>16</sub> OA experimental design

| Experimental No | Variables and their levels |                    |        |                    |
|-----------------|----------------------------|--------------------|--------|--------------------|
|                 | A: CD                      | B: pH <sub>i</sub> | C: RSE | D: PS <sub>i</sub> |
| 1               | 1                          | 1                  | 1      | 1                  |
| 2               | 1                          | 2                  | 2      | 2                  |
| 3               | 1                          | 3                  | 3      | 3                  |
| 4               | 1                          | 4                  | 4      | 4                  |
| 5               | 2                          | 1                  | 2      | 3                  |
| 6               | 2                          | 2                  | 1      | 4                  |
| 7               | 2                          | 3                  | 4      | 1                  |
| 8               | 2                          | 4                  | 3      | 2                  |
| 9               | 3                          | 1                  | 3      | 4                  |
| 10              | 3                          | 2                  | 4      | 3                  |
| 11              | 3                          | 3                  | 1      | 2                  |
| 12              | 3                          | 4                  | 2      | 1                  |
| 13              | 4                          | 1                  | 4      | 2                  |
| 14              | 4                          | 2                  | 3      | 1                  |
| 15              | 4                          | 3                  | 2      | 4                  |
| 16              | 4                          | 4                  | 1      | 3                  |

characteristic for PS and TOC removal was selected as "larger the better" in the present study. The anticipated outcome for the optimization technique is the maximum if "bigger is better." The S/N ratio can be determined using the expressions provided by authors in earlier studies (Kumar & Basu, 2023; Gokkus et al., 2012). Based on the OA design results, the Taguchi prediction technique used an additive model to predict the response at optimum working conditions (Khorshidi et al., 2015; Taguchi, 1986). The confidence interval (CI) is calculated to assess the adequacy of verification trials. The formula can be used to compute CI, as described by Gunes et al., (2011). The additive model is only adequate if the predicted outcomes are within these ranges (Irdemez et al., 2006).

ANOVA was used to justify the experimental theories of statistical study. The statistics, namely degree of freedom (DOF), sums of squares (SS), adjusted means of squares, *F*-value, error and *P*-value were studied. The *F*-test and ANOVA was employed to evaluate the statistical validity of the model equation and model terms (Jadhav et al., 2014). The quantitative evaluation of each operating variable for PS and TOC removal has been determined using ANOVA. A quantitative assessment of each operating variable determined by percentage contribution has been discussed by Taguchi, (1986).

### 3 Results and discussion

#### 3.1 One variable at a time (OVAT) experimental analysis for PS removal

##### 3.1.1 Effects of initial pH of solution on EC and EC-EO practices

Typically, pH is a crucial factor that can significantly alter the efficacy of an electrochemical process. In order to investigate the effects of pH<sub>i</sub> on the TOC (RE<sub>TOC</sub>) and PS (RE<sub>PS</sub>) removal efficiency via EC and EC-EO processes, the pH<sub>i</sub> was changed from 3–7 using 1/10N NaOH and 1/10N HCl solutions. The CD, PS<sub>i</sub> and RSE were maintained at 4.75 mA.cm<sup>-2</sup>, 0.5 g/L and 0 rpm, respectively.

The Fig. 2a shows that the TOC and syntan removal substantially depend on the pH<sub>i</sub> of the synthetic wastewater in the EC process.

It was noticed that the RE<sub>TOC</sub> and RE<sub>PS</sub> from water decreased as the pH became more acidic or alkaline. The findings indicate that as the pH<sub>i</sub> rose from 3 to 4, after 90 min of ET, the RE<sub>TOC</sub> and RE<sub>PS</sub> increased from 61.18% to 64.23% and 60.77% to 73.83%, respectively. As the pH<sub>i</sub> rose from 4 to 7, the RE<sub>TOC</sub> and RE<sub>PS</sub> dropped by -16.21% and -15.9%, respectively. The Predominance-zone diagram (PZD) explains this anticipated behavior. PZD states that Al(OH)<sup>4-</sup> is the species for aluminum in highly alkaline conditions. Poor coagulation is exhibited by

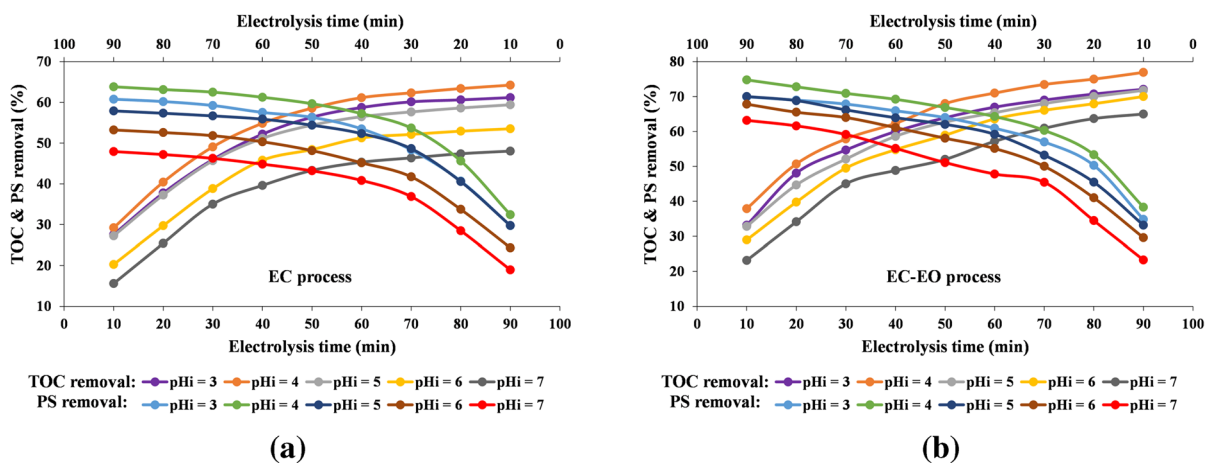


**Fig. 2** Effects of initial pH on the elimination of TOC and phenolic syntan by (a) EC practice and (b) EC-EO practice [CD=4.75 mA/cm.<sup>2</sup>; NaCl=2 g/L; RSE=0 rpm; PS<sub>i</sub>=0.5 g/L]

these species (Kim et al., 2002). Aluminum cations generated at the anode produced the polymeric species  $\text{Al}_{13}\text{O}_4(\text{OH})_{24}^{7+}$  and precipitated  $\text{Al}(\text{OH})_3$ , enabling the coagulation to be more successful when conducted in a slightly acidic environment (Holt et al., 2002), as supported by the Eqs. (1–3). If NaCl is present in the solution, a secondary reaction might precede at a high potential producing oxidizing agents ( $\text{OCI}^-$ ,  $\text{Cl}_2$  and  $\text{HOCl}$ ) throughout the EC process (Adhoum & Monser, 2004; Kobya et al., 2003). These species are capable of oxidizing organic matter and promoting electrode reactions.

A crucial factor in EC-EO is the  $\text{pH}_i$  of the solution due to its direct impact on the production of electroactive oxidizing ( $\text{Cl}_2$ ,  $\text{HOCl}$ , and  $\text{OCI}^-$ ) and coagulative ( $\text{Al}(\text{OH})_3$ ) species (Fajardo et al., 2017; Holt et al., 2002; Jin et al., 2014). Additionally, the oxygen evolution process, a side reaction, is significantly impacted by the pH. As shown in Fig. 2b, the  $\text{RE}_{\text{TOC}}$  and  $\text{RE}_{\text{PS}}$  for chosen  $\text{pH}_i$  values at the end of 90 min were as follows:  $\text{pH}_i$  3 (72.07% and 69.94%) <  $\text{pH}_i$  4 (76.93% and 74.8%) >  $\text{pH}_i$  5 (71.77% and 70%) >  $\text{pH}_i$  6 (70% and 67.83%) >  $\text{pH}_i$  7 (65% and 63.17%). At  $\text{pH}_i$  4, the highest  $\text{RE}_{\text{TOC}}$  and  $\text{RE}_{\text{PS}}$  were observed. In contrast to the initial pH (4) of the untreated wastewater, the experimental findings revealed that the final pH varied from 5 to 7 in the treated wastewater. It is apparent that  $\text{Cl}_2(\text{aq})$  ( $\text{pH} < 5$ ) and  $\text{HClO}$  ( $5 < \text{pH} < 7$ ) formed as the predominant electroactive oxidant entities in an acidic environment have a more noticeable impact on  $\text{RE}_{\text{TOC}}$  and  $\text{RE}_{\text{PS}}$  than  $\text{ClO}^-$  generated at  $\text{pH} > 8$ . This is because  $\text{ClO}^-$  (0.89 V) and  $\text{Cl}_2$  (1.36 V) have lower standard oxidation potentials than  $\text{HClO}$  (1.49 V) (Fajardo et al., 2017). The wastewater pH is known to strongly influence the proportions of  $\text{HClO}$  and  $\text{ClO}^-$  in the solution (Anglada et al., 2010; Mandal et al., 2017). Low pH promotes phenolic sytan removal while decreasing unwanted oxygen evolution reactions (side reactions) that consume some of the electric energy (Feng & Li, 2003; Li et al., 2017; Wu & Zhou, 2001). In an acidic medium,  $\text{Al}(\text{OH})_3$  flocs are simultaneously generated (as discussed above), aiding in removing pollutants from the wastewater. Chlorine transforms into the low-oxidation potential chlorate ( $\text{ClO}_3^-$ ) ion at high pH levels (Anglada et al., 2010; Mandal et al., 2017). At this time,  $\text{Al}(\text{OH})^{4+}$  species with

weak coagulation characteristics are also generated in alkaline pH (as discussed above). Therefore, high pH was unfavourable for the removal of phenolic sytan from the synthetic wastewater by the EC-EO process.

### 3.1.2 Effects of Rotational speed of electrode on EC and EC-EO process

Many experimental trials were conducted with various RSE (0, 40, 70, and 100 rpm) levels to determine the impacts of RSE on the  $\text{RE}_{\text{TOC}}$  and  $\text{RE}_{\text{PS}}$  via the EC and EC-EO processes, as indicated in the Fig. 3. Other variables were set to  $\text{PS}_i = 0.5 \text{ g.L}^{-1}$ ,  $\text{pH}_i = 4$  and  $\text{CD} = 4.75 \text{ mA.cm}^{-2}$ . The Reynolds number ( $R_e$ ) was used to determine the flow state within the electrochemical cell due to the RSE (Eq. 15). The Reynolds number was calculated as  $9.1 \times 10^4$ ,  $15.9 \times 10^4$  and  $22.75 \times 10^4$ , corresponding to RSE of 40, 70 and 100 rpm, respectively. It suggests that the flow in the electrochemical reactor was turbulent ( $R_e > 104$ ), which might have helped to prevent the accumulation of hydrogen and oxygen bubbles at the electrode or reduce the chances of electrode passivation (Miriam et al., 2019).

$$R_e = \rho N d^2 / \mu \quad (15)$$

where  $\rho$  = fluid density ( $\text{g/cm}^3$ ),  $N$  = rotational speed (rpm),  $\mu$  = fluid viscosity ( $\text{g/cm}\cdot\text{s}$ ) and  $d$  = effective diameter of the anode (cm).

Figure 3a shows that the  $\text{RE}_{\text{TOC}}$  and  $\text{RE}_{\text{PS}}$  increased from 64.23 to 71.28% and 63.83 to 70.52% as the RSE value increased from 0 to 70 rpm after 90 min of ET in the EC process. When the RSE was further increased from 70 to 100 rpm, the  $\text{RE}_{\text{TOC}}$  and  $\text{RE}_{\text{PS}}$  decreased to 62.32% and 59.6%, respectively. The maximum  $\text{RE}_{\text{TOC}}$  and  $\text{RE}_{\text{PS}}$  were observed at 70 rpm. So, the optimum RSE was considered as 70 rpm for TOC and PS removal by the EC method.

Figure 3b shows the impact of RSE on the  $\text{RE}_{\text{TOC}}$  and  $\text{RE}_{\text{PS}}$  by the EC-EO process using the composite anode. At 0 rpm, after an ET of 90 min, the values of  $\text{RE}_{\text{TOC}}$  and  $\text{RE}_{\text{PS}}$  were 76.93% and 74.8%, respectively. As the RSE was raised from 0 to 70 rpm during the first phase, pollutant removal efficiency was noted to be improved. At the RSE of 70 rpm, after 90 min of ET, the maximum



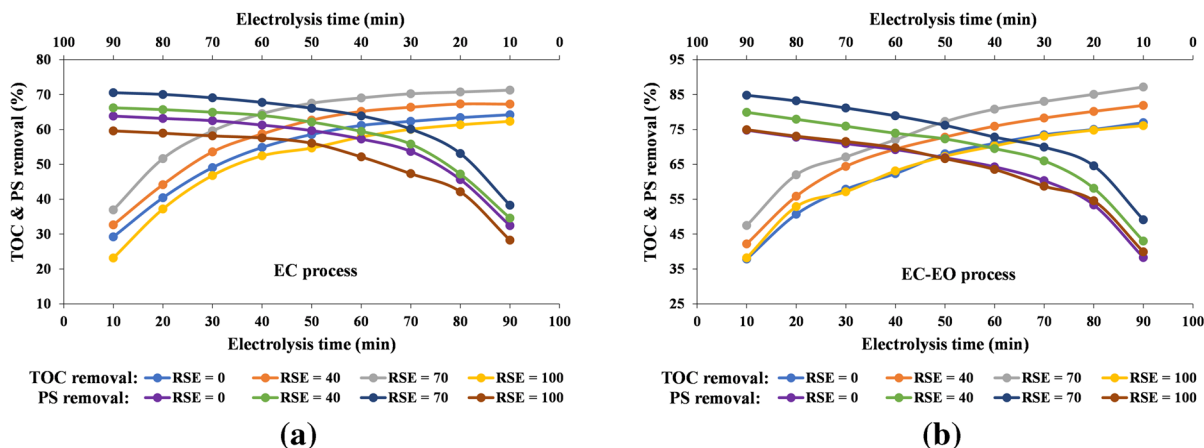


**Fig. 3** Effects of rotational speed of electrode on the elimination of TOC and phenolic syntan by (a) EC practice and (b) EC-EO practice: [CD=4.75 mA/cm<sup>2</sup>; NaCl=2 g/L; pH<sub>i</sub>=4; PS<sub>i</sub>=0.5 g/L]

RE<sub>TOC</sub> and RE<sub>PS</sub> were 87.17% and 84.83%, respectively. However, the decrease in RE<sub>TOC</sub> (87.17% to 76.07%) and RE<sub>PS</sub> (84.83% to 74.92%) was noted after the rotating speed was increased from 70 to 100 rpm. It was confirmed that the EC-EO process was superior to the EC approach. The results showed that at optimum rpm, the RE<sub>TOC</sub> and RE<sub>PS</sub> increased by +15.89% and +14.31% in the EC-EO process, as compared to the EC process.

The pollutant removal efficiency rises after at the optimum RSE. Raising the anode rotation speed would result in the assimilation of flocs formed by Al(OH)<sub>3</sub>, causing the coagulant precipitation to become faster. The RSE was kept high enough to effectively disperse the coagulant species, oxidizing species, OH<sup>-</sup>, pH and maintain uniform in-situ temperature resulting in increased homogeneity in the wastewater within the reactor (Karthikeyan et al., 2014). In addition to favouring the anodic oxidation reactions, high RSE may decrease the diffusion-controlled cathodic reduction of hypochlorite (El-Ashtouky et al., 2009). However, raising the RSE above the optimal level causes the flocs to disintegrate due to hydrodynamic shear, which desorbs the contaminants that have been adsorbed (Kumar & Basu, 2022a, b). Because of their tiny size and poor settling properties, these disintegrating flocs can be challenging to remove by gravity settling from wastewater (Aber et al., 2006). Fewer contaminants are

adsorbed on the electrode surface as the rotating speed increases, resulting in a diminished electrode oxidizing capability, leading to reduced pollutant removal efficiency (Luu, 2020).

### 3.1.3 Effects of current density on EC and EC-EO practices

The current density, or current per unit area of the electrode, is a vital factor for controlling the rate of electrochemical reactions (Chen, 2004). CD has a direct impact on the amount of metal emitted into the solution and the formation of bubbles in the EC method, as well as the rate of generation of oxidizing species (Cl<sub>2</sub>, HOCl, and OCl<sup>-</sup>) in the EO technique (Chen, 2004; Fajardo et al., 2017). Therefore, current density regulates the rates at which coagulant and oxidizing species form electrolytically in EC-EO processes. Thus, the pollutants removal rates should be significantly impacted by this parameter. EC and EC-EO processes were operated to assess the effects of CD on RE<sub>TOC</sub> and RE<sub>PS</sub> at CD ranges of 2.375–14.25 mA/cm<sup>2</sup>, as shown in Figs. 4a and b. Other variables were set to pH<sub>i</sub> of 4, RSE of 70 rpm and PS<sub>i</sub>=0.5 g.L<sup>-1</sup>. The findings demonstrate that TOC and PS removal efficiency in the EC process improved with an increase in the CD. After 90 min of ET, the RE<sub>TOC</sub> and RE<sub>PS</sub> for particular CD applications were attained as: 2.375 mA/cm<sup>2</sup> (57.3% and 56%) < 4.75 mA/cm<sup>2</sup>

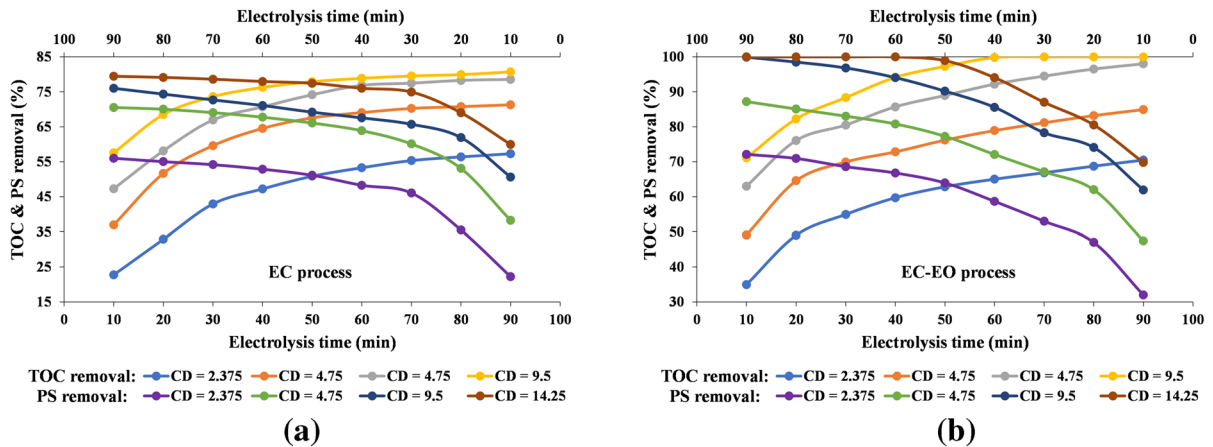


**Fig. 4** Effects of CD on the elimination of TOC and phenolic syntan by (a) EC practice and (b) EC-EO practice: [pH<sub>i</sub>=4; NaCl=2 g/L; RSE=70 rpm; PS<sub>i</sub>=0.5 g/L]

(71.28% and 70.53%) < 9.5 mA/cm<sup>2</sup> (78.53% and 75.63%). This behavior can be explained because anode disintegration to Al<sup>3+</sup> ions improved as CD increased. As a result of the hydrolysis of Al<sup>3+</sup> ions, aluminum hydroxides are formed, producing more sludge and significantly removing contaminants via adsorption on Al(OH)<sub>3</sub> and its polymeric complexes (Guo et al., 2006). Additionally, the cathode produces greater hydrogen bubbles, which improves the mixing rate of aluminum hydroxides and ions and flotation ability of the reactor, increasing the removal efficiency (Heidmann and Calmano). Moreover, it has already been observed that the size of the bubble reduces with rising CD (Khosla et al., 1991), which is advantageous to the removal process. Therefore, the CD controls the amount of coagulant formation at the anode and the rate and size of H<sub>2</sub> and O<sub>2</sub> bubble production at the cathode. It was observed that at high CD, the rate of pollution removal rises initially and subsequently falls as the electrolysis time increases. At CD of 14.25 mA/cm<sup>2</sup>, ET of 60 min, the RE<sub>TOC</sub> and RE<sub>PS</sub> were found to be 78.86% and 77.94%, respectively. But a CD of 9.5 mA/cm<sup>2</sup> would take an ET of 90 min to attain the same removal efficiency. However, the optimum CD must be considered at the highest removal efficiency of pollutants, lowest operational costs and energy consumption. Figure 4a and 5a observed that when CD increased from 9.5 mA.cm<sup>-2</sup> to 14.25 mA.cm<sup>-2</sup>, a marginal increase in RETOC (+2.17%) and REPS

(+3.43%) were found after ET of 90 min, and it also increased energy consumption (+53.27% and +52% for per gram TOC and PS removal). The OC (calculated by Eq. 22) for applied current densities of 2.375, 4.75, 9.5 and 14.25 mA/cm<sup>2</sup> were 0.29, 0.61, 1.66 and 2.90 USD/m<sup>3</sup>, respectively, and shown in Fig. 5a. This is due to the expected additional reaction at the anode in conjunction with the anodic dissolution of ions when CD is increased (Adhoum & Monser, 2004; Kobya et al., 2003). These additional reactions result in oxygen evolution and the generation of hypochlorite ions from the oxidation of chloride ions at the anode increases (Adhoum & Monser, 2004; Kobya et al., 2003). The subsequent elimination of pollutants is probably due to these hypochlorite ions. The secondary reactions increase the ohmic potential drop, which lowers the current efficiency of anodic dissolution of aluminum (Mansouri et al., 2011). Figure 5a shows that with an increase in CD from 2.375 to 14.25 mA/cm<sup>2</sup>, ohmic drop (calculated by Eq. 13) increased from 0.0024 to 0.0143 Ω and CE decreased from 109 to 97%, after 90 min of ET.

The performance of the EC-EO method was explored at varied CD with a composite rotating electrode, as illustrated in Fig. 4b. The oxidant species (Cl<sub>2</sub>, HClO and OCl<sup>-</sup>) and coagulant (Al(OH)<sub>3</sub>) are expected to be formed simultaneously, as shown in Eqs. 4–9. In the reactor, Al(OH)<sub>3</sub> is formed through the neutralization of negatively charged colloids. Similarly, oxidant species formed

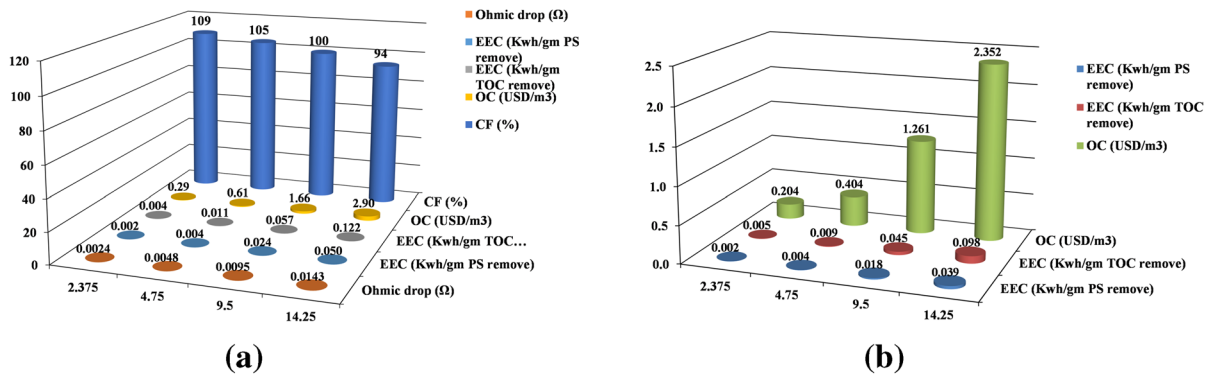


**Fig. 5** **a** Effects of CD on Operating cost, energy consumption per gram pollutant remove, ohmic drop and current efficiency in EC process and **b** Effects of current density on operating cost and energy consume per gram pollutants remove in EC-EO process

through indirect oxidation react and degrade dissolved organic matter. A better aggregation of colloidal particles is promoted by the indirect action of HClO on hydrophilic colloids. After the aggregation of colloidal particles resulting from  $Al^{3+}$  action, wastewater treatment occurs. The TOC and PS removal directly rely on current density, as seen in Fig. 4b. After 90 min of ET, the  $RE_{TOC}$  and  $RE_{PS}$  for the specified CD were as follows: 2.375 mA/cm<sup>2</sup> (72.10% and 70.4%) < 4.75 mA/cm<sup>2</sup> (87.17% and 85%) < 9.5 mA/cm<sup>2</sup> (99.9% and 98%). The most noticeable difference in the  $RE_{TOC}$  and  $RE_{PS}$  for all four different CD values was seen towards the middle of the 90-min ET. The variation in removal efficiency during these minutes may exceed 1.5 times. At 60 min, 66.75% TOC and 65% PS removal efficiencies were attained at 2.375 mA/cm<sup>2</sup>; whereas, very high TOC (100%) and PS (99.8%) removal efficiencies were achieved at 14.25 mA/cm<sup>2</sup>. It is clear that there is rise in  $RE_{TOC}$  and  $RE_{PS}$  with increasing CD and high CD values result in a shorter ET for maximum removal, compared to low CD values. This phenomenon may be attributed to the fact that more coagulant and oxidant species are produced at high current densities, which is significantly greater than the oxygen evolution potential of the electrode (Geng et al., 2010; Govindaraj et al., 2010). As the current density decreases, the anode potential falls below the electrode potential essential for the partial oxidation reaction (Fernandes et al., 2016). However, CD increases from 9.5 to 14.25 mA/cm<sup>2</sup>, an insignificant rise in  $RE_{TOC}$  (+3%) and  $RE_{PS}$  (+5%) at the end of 70 min ET. This showed that

as the CD improved, the  $RE_{TOC}$  and  $RE_{PS}$  increment rates would no longer be significant. This is due to higher CD that can cause a violent water discharge with the formation of a higher amount of oxygen and hydrogen bubbles. This can further restrict the anode dissolution rate and limit the production of oxidant species (Benhadji et al., 2011; Mansouri et al., 2011). As shown in Fig. 5b, the EEC and OC values depend on the applied CD, indicating that both values rise concurrently with an increase in CD. The EEC and OC values were determined to be minimum at 2.375 mA/cm<sup>2</sup> and maximum at 14.25 mA/cm<sup>2</sup>, respectively. At the end of 90 min, the difference between the  $RE_{TOC}$  and  $RE_{PS}$  at the lowest (2.375 mA/cm<sup>2</sup>) and highest (14.25 mA/cm<sup>2</sup>) CD was around 28–29%, with an increase in OC of 10–11 times. However, these factors must be kept as low as possible to provide low-cost treatment. So, CD must be optimized for maximum removal of pollutants at the lowest OC.

#### 3.1.4 Effects of initial amount of phenolic syntan on EC and EC-EO process

In case of real industrial wastewaters, there is a wide variation in the concentration of pollutants released into the wastewaters from different manufacturing operations. Therefore, it is essential to investigate the effect of varying initial PS concentrations on the performance of the EC and EC-EO approaches. The impact of varying  $PS_i$  (0.25–1.5 g/L) on the  $RE_{TOC}$  and  $RE_{PS}$  via the EC and EC-EO processes was investigated at a given operating condition: CD

of 14.25 mA/cm<sup>2</sup>, pH<sub>i</sub> of 4 and RSE of 70 rpm. The results have been shown in Figs. 6a and b.

In the EC method, the RE<sub>TOC</sub> and RE<sub>PS</sub> were influenced by electrolysis time and PS<sub>i</sub>. The maximum RE<sub>TOC</sub> and RE<sub>PS</sub> were observed at PS<sub>i</sub>=0.25 g/L. At higher PS<sub>i</sub> (1.5 g/L) values, the RE<sub>TOC</sub> (-16.87%) and RE<sub>PS</sub> (-18%) reduced after 90 min of ET. Adsorption of pollutants on the surface of the Al(OH)<sub>3</sub> flocs is among most effective mechanisms for pollutant removal in the EC process (Holt et al., 2002). Faraday's law states that at a fixed CD and electrolysis period, a constant amount of Al cations will be emitted into the aqueous solution for different PS<sub>i</sub> (Afroze & Sen, 2018). Thus, the same number of flocs will develop in the solution under various PS<sub>i</sub>. A specific number of flocs are able to adsorb a certain amount of pollutants because of the limited availability of adsorption sites (Ghalwa et al., 2012). Thus, as PS<sub>i</sub> rises, RE<sub>TOC</sub> and RE<sub>PS</sub> is expected to reduce.

The treatment efficiency of the EC-EO method can be influenced by the initial PS concentration and electrolysis period. The treatment period controls the formation rate of oxidant species and Al<sup>+3</sup> ions. Complete removal of the TOC and PS was observed at 0.25 g/L after 50 min of ET. Fifty minutes of ET was observed to be necessary to generate a significant number of oxidant species and Al<sup>+3</sup> ions. At comparatively large quantities of phenolic sytan (0.5, 1.0, and 1.5 g/L), the RE<sub>TOC</sub> and RE<sub>PS</sub> were 100% and 98.8% at 70 min ET, 100% and 98.07% at 80 min, and 88.45% and 86.83% at 90 min ET, respectively. At

fixed CD and ET, a fixed amount of oxidant and coagulant species would be released. Since fewer oxidant and coagulant species would be available for treatment of high PS<sub>i</sub>, a greater electrolysis time would be required for maximum removal. This could be due to the limited interaction among the sytan molecules and the oxidants and coagulant species (HClO, Cl<sub>2</sub>, OCl<sup>-</sup> and aluminum hydroxide complexes) formed in-situ during the EC-EO process (Adhoum & Monser, 2004; Dirany et al., 2012). At this current density, the oxidant and coagulant species generated are insufficient to completely remove the higher PS<sub>i</sub>.

### 3.2 Taguchi optimization study

#### 3.2.1 Taguchi outcomes

The optimal working conditions for the EC and EC-EO practices were determined using the Taguchi approach. It identified the operating parameters that have the greatest influence on TOC and PS removal. This study used Taguchi L<sub>16</sub> OA (4<sup>4</sup>) with four variables and four levels for batch experimental analysis. The experimental results of the EC and EC-EO processes for Taguchi L<sub>16</sub> OA have been shown in Figs. 7a&b.

The results of the Taguchi experimental study are transformed into an S/N ratio. The S/N ratio is a qualitative indicator that determines the effect of varying a particular factor on process performance. Figure 7a&b shows the computed S/N ratio values

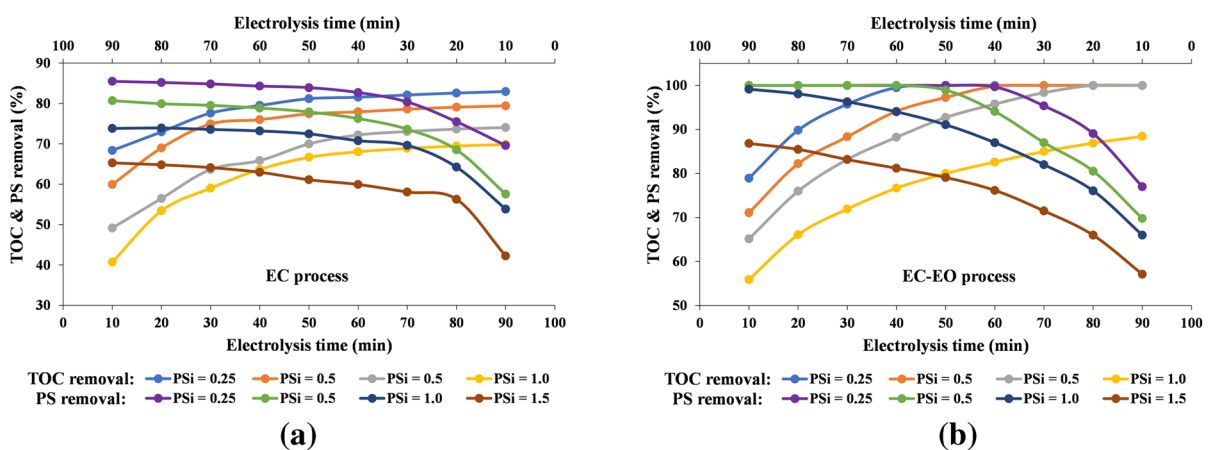


**Fig. 6** Effects of Initial amount of PS on the elimination of TOC and phenolic sytan by (a) EC practice and (b) EC-EO practice: [pH<sub>i</sub> = 4; NaCl = 2 g/L; RSE = 70 rpm; CD = 14.25 mA/cm<sup>2</sup>]

for  $RE_{TOC}$  and  $RE_{PS}$  by the EC and EC-EO processes. The larger-the-better performance equation was chosen as the objective function in this study because the maximum  $RE_{TOC}$  and  $RE_{PS}$  were measured. The mean value of the S/N ratio for a specific level for each variable was calculated using the analysis of means (ANOM). The ANOM outcomes are displayed in Table 5. The parameters were ranked according to their Delta values. These values have been calculated by subtracting highest and lowest averages of each parameter. Ranking would make it easier to compare the relative magnitude of the impact of a factor on the response. The rank would be greater as the higher the Delta value. In the EC process, ranks 1, 2, 3, and 4 have been allocated to the CD,  $PS_i$ ,  $pH_i$  and RSE for TOC and PS removal. In the EC-EO process, CD has

been given rank 1, whereas,  $PS_i$ , RSE, and  $pH_i$  have been given ranks 2, 3, and 4, respectively, for TOC and PS removal. Figures 8a&b depicts the major impacts of operational factors on S/N ratios in the EC and EC-EO techniques. The S/N ratio value was employed to determine the optimum working condition, where the greatest S/N ratio value of the parameter level was noted for significant optimal results. The optimum value was determined to be the greatest S/N ratio value. According to Fig. 8a, the parameter-level combination of optimal operating conditions for TOC and PS removal by the EC process was found to be A4, B2, C3 and D1. i.e., CD (14.25 mA/cm<sup>2</sup>),  $pH_i$  (4), RSE (70 rpm) and  $PS_i$  (0.25 g/L). A similar trend of optimum conditions for TOC and PS removal by EC-EO practice is shown in Fig. 8b.

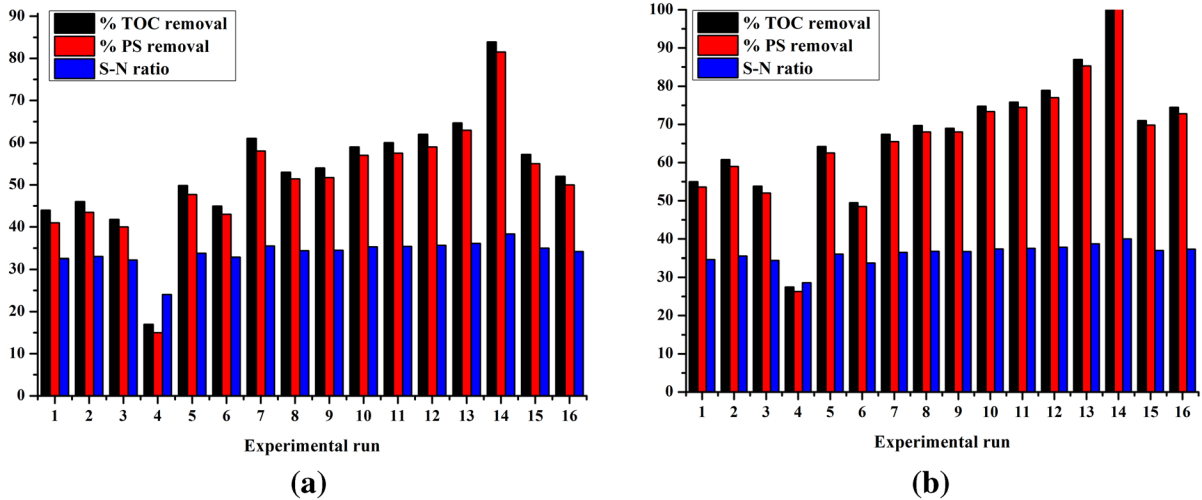


Fig. 7 Experimental outcomes of (a) EC and (b) EC-EO practice for Taguchi  $L_{16}$  OA

Table 5 ANOM results for S/N ratio for EC and EC-EO process

| Level | EC process  |        |       |        |                |        |       |        | EC-EO process |        |       |        |                |        |       |        |
|-------|-------------|--------|-------|--------|----------------|--------|-------|--------|---------------|--------|-------|--------|----------------|--------|-------|--------|
|       | TOC removal |        |       |        | PS degradation |        |       |        | TOC removal   |        |       |        | PS degradation |        |       |        |
|       | CD          | $pH_i$ | RSE   | $PS_i$ | CD             | $pH_i$ | RSE   | $PS_i$ | CD            | $pH_i$ | RSE   | $PS_i$ | CD             | $pH_i$ | RSE   | $PS_i$ |
| 1     | 30.79       | 34.42  | 33.95 | 35.72  | 30.15          | 34.02  | 33.52 | 35.29  | 33.47         | 36.63  | 35.93 | 37.33  | 33.18          | 36.44  | 35.75 | 37.16  |
| 2     | 34.30       | 35.05  | 34.55 | 34.88  | 33.93          | 34.69  | 34.14 | 34.54  | 35.87         | 36.76  | 36.7  | 37.23  | 35.65          | 36.61  | 36.49 | 37.03  |
| 3     | 35.37       | 34.71  | 35.01 | 34.03  | 35             | 34.33  | 34.69 | 33.68  | 37.45         | 36.45  | 37.06 | 36.42  | 37.28          | 36.24  | 36.91 | 36.20  |
| 4     | 36.04       | 32.32  | 32.99 | 31.87  | 35.75          | 31.78  | 32.47 | 31.32  | 38.31         | 35.26  | 35.41 | 34.12  | 38.18          | 35.01  | 35.16 | 33.91  |
| Delta | 5.25        | 2.74   | 2.02  | 3.86   | 5.60           | 2.91   | 2.22  | 3.97   | 4.84          | 1.5    | 1.66  | 3.21   | 5.00           | 1.6    | 1.74  | 3.52   |
| Rank  | 1           | 3      | 4     | 2      | 1              | 3      | 4     | 2      | 1             | 4      | 3     | 2      | 1              | 4      | 3     | 2      |

### 3.2.2 ANOVA outcomes

Table 6 displays the results of the ANOVA test for the removal of TOC and PS in the EC and EC-EO methods, respectively. The ANOVA analysis used Fisher's test ( $F$ -value) to estimate the qualitative impact of each variable on the responses. The higher  $F$ -value denotes that the factors adequately describe the variation in the data about its mean (Karthikeyan et al., 2014). At a 95% confidence level, the  $F$ -test was performed for each parameter. The  $F$ -ratio can identify the factors that significantly affect the  $RE_{TOC}$  and  $RE_{PS}$ . A high  $F$ -value of CD (1399.69 and 1077.84) had the most significant influence on TOC and PS removal by the EC process. Similarly, in the EC-EO process, CD has a larger  $F$ -value (1096.80 and 2547.21),

resulting in the most significant influence on the  $RE_{TOC}$  and  $RE_{PS}$ . The  $p$ -value, employed to identify whether parameters had a substantial impact on the responses, is another statistical tool useful for qualitative analysis in an ANOVA. The degree of confidence is represented by the  $p$ -value. When the  $p$ -value was less than 0.05, the degree of statistical was high (Garcia et al., 2013). According to  $p$ -values at the 95% confidence level, all of the parameters in this investigation (CD,  $pH_i$ , RSE, and  $PS_i$ ) had a statistically significant ( $P$ -value < 0.05) impact on the  $RE_{TOC}$  and  $RE_{PS}$  by the EC and EC-EO techniques.

In ANOVA analysis, the percentage contribution (CR%) is helpful for the quantitative assessment of the factorial impacts of the performance indicators. Table 6 displays the percentage contributions

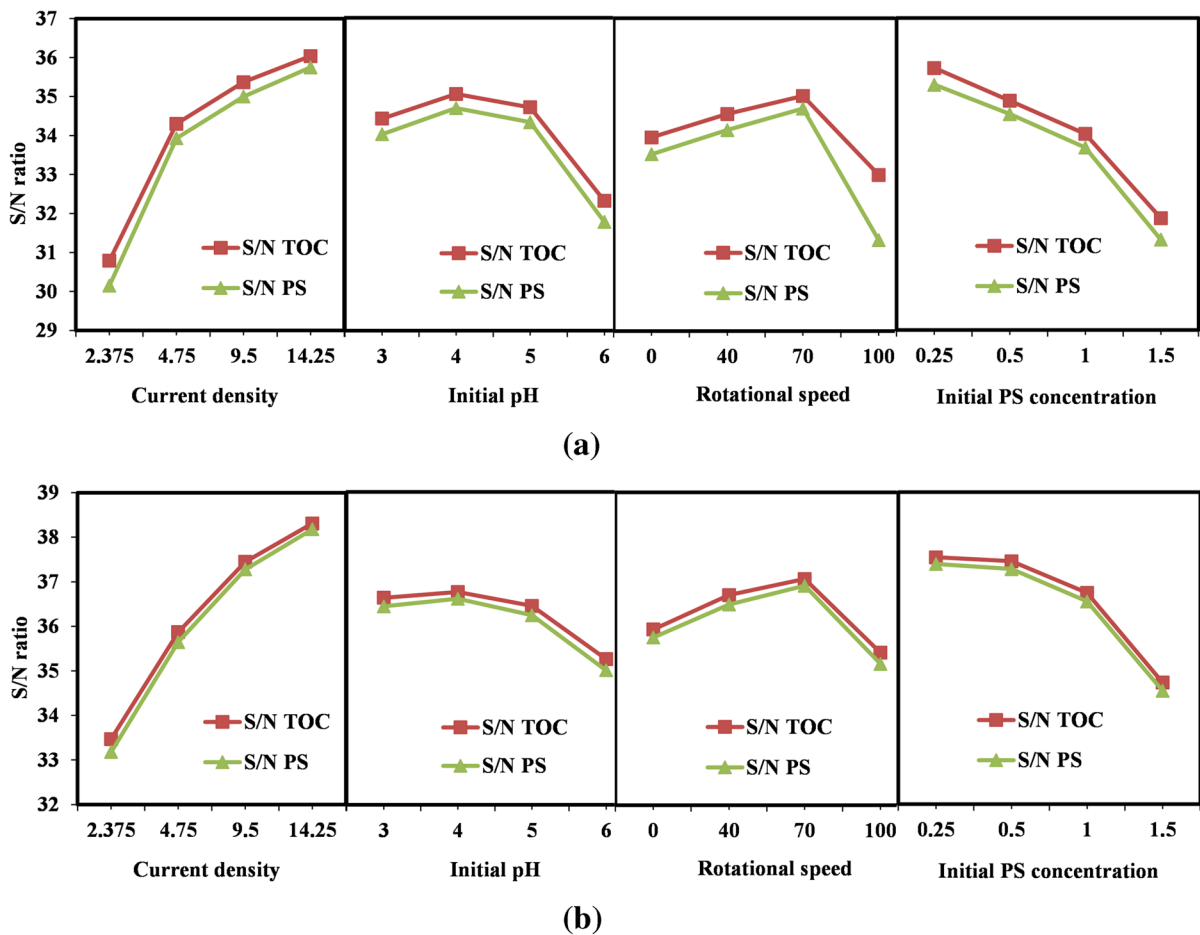


**Fig. 8** Main impacts for S/N ratios for (a) EC method and (b) EC-EO process

**Table 6** ANOVA results for the removal of TOC and PS by EC and EC-EO processes

| EC Process      | TOC removal |         |         |        |         |         |         | PS degradation |         |        |         |         |         |
|-----------------|-------------|---------|---------|--------|---------|---------|---------|----------------|---------|--------|---------|---------|---------|
|                 | Source      | DF      | Seq SS  | Adj MS | CR (%)  | F-value | P-value | DF             | Seq SS  | Adj MS | CR (%)  | F-value | P-value |
| CD              | 3           | 1657.40 | 552.467 | 55.86  | 1399.69 | 0.000   | 3       | 1672.88        | 557.628 | 57.09  | 1077.84 | 0.000   |         |
| pH <sub>i</sub> | 3           | 331.28  | 110.428 | 11.17  | 279.77  | 0.000   | 3       | 325.21         | 108.404 | 11.10  | 209.54  | 0.001   |         |
| RSE             | 3           | 166.01  | 55.336  | 5.60   | 140.20  | 0.001   | 3       | 175.76         | 58.586  | 6.00   | 113.24  | 0.001   |         |
| PS <sub>i</sub> | 3           | 811.01  | 270.336 | 27.34  | 684.90  | 0.000   | 3       | 754.85         | 251.617 | 25.76  | 486.35  | 0.000   |         |
| Error           | 3           | 1.18    | 0.395   | 0.04   |         |         | 3       | 1.55           | 0.517   | 0.05   |         |         |         |
| Total           | 15          | 2966.88 |         | 100    |         |         | 15      | 2930.26        |         | 100    |         |         |         |
| EC-EO process   | TOC removal |         |         |        |         |         |         | PS degradation |         |        |         |         |         |
|                 | Source      | DF      | Seq SS  | Adj MS | CR (%)  | F-value | P-value | DF             | Seq SS  | Adj MS | CR (%)  | F-value | P-value |
| CD              | 3           | 2597.91 | 865.969 | 73.69  | 1096.80 | 0.000   | 3       | 2659.85        | 886.616 | 64.28  | 2547.21 | 0.000   |         |
| pH <sub>i</sub> | 3           | 158.72  | 52.906  | 3.89   | 67.01   | 0.003   | 3       | 178.48         | 59.494  | 4.31   | 170.92  | 0.001   |         |
| RSE             | 3           | 235.20  | 78.400  | 5.77   | 99.30   | 0.002   | 3       | 247.81         | 82.604  | 5.99   | 237.32  | 0.000   |         |
| PS <sub>i</sub> | 3           | 1084.62 | 361.540 | 26.59  | 457.91  | 0.000   | 3       | 1050.86        | 350.286 | 25.40  | 1006.36 | 0.000   |         |
| Error           | 3           | 2.37    | 0.790   | 0.06   |         |         | 3       | 1.04           | 0.348   | 0.03   |         |         |         |
| Total           | 15          | 4078.81 |         | 100    |         |         | 15      | 4138.04        |         | 100    |         |         |         |

of each factor to the TOC and PS removal by the EC and EC-EO techniques. In case of the EC process, the CR% of the parameters for TOC removal was noted to be in the following order: CD (58.86%) > PS<sub>i</sub> (27.24%) > pH<sub>i</sub> (11.17%) > RSE (5.6%) and for the PS removal was found to be in the following order: CD (57.09%) > PS<sub>i</sub> (25.76%) > pH<sub>i</sub> (11.10%) > RSE (6.0%). Similarly, in the EC-EO process, the CR% of the parameters for TOC removal was observed to be in the following order: CD (63.69%) > PS<sub>i</sub> (26.59%) > RSE (5.77%) > pH<sub>i</sub> (3.89%) and for the PS removal was in the following order: CD (64.28%) > PS<sub>i</sub> (25.4%) > RSE (5.99%) > pH<sub>i</sub> (4.31%).

Figure 9a&b depicts the correlation between the actual and predicted values of RE<sub>TOC</sub> and RE<sub>PS</sub> in the EC and EC-EO processes. The R<sup>2</sup> values for TOC and PS removal in the EC process were 0.9996 and 0.9995, respectively. Similarly, the R<sup>2</sup> value for TOC and PS removal in the EC-EO process was 0.9995 and 0.9998, respectively. This confirmed a strong correlation between the experimental and predicted values.

### 3.2.3 Confirmation experiment

The final stage of the Taguchi method comprises of the confirmation experiment. The confirmation test is essential to verifying the experimental results. Once the optimal working conditions were found and the responses were predicted within these conditions, an

additional trial was constructed and performed using optimal value or operational factors. Table 7 shows the results of EC and EC-EO practices under optimal operating settings. Thus, the predicted value was evaluated using the additive model to clarify the result. It demonstrates that the predicted response of the additive model to the EC and EC-EO processes was within the CI.

The additive model and verification experiment also obtained a difference between the RE<sub>TOC</sub> and RE<sub>PS</sub> of less than 5%. Hence, the experimental and predicted values showed a strong correlation, with minimal interactive effects between parameters. The verification experiment could effectively determine the appropriateness of the additive model. Table 7 demonstrates that the EC-EO method performed significantly better than the EC procedure. In the EC-EO process, 100% TOC and PS removals with lowest EEC (0.113 kWh/g TOC removed and 0.0453 kWh/g PS removed) was observed. Likewise, in the EC process, 84.36% TOC and 81.96% PS removals with an EEC of 0.135 kWh/g TOC removed and 0.056 kWh/g PS removed was noted. The EC-EO method showed to have a lower operational cost (-19.65%) compared to the EC process.

### 3.3 UV-VIS and FT-IR study

The degradation of PS in the electrochemical process was investigated by analyzing the samples in an UV/

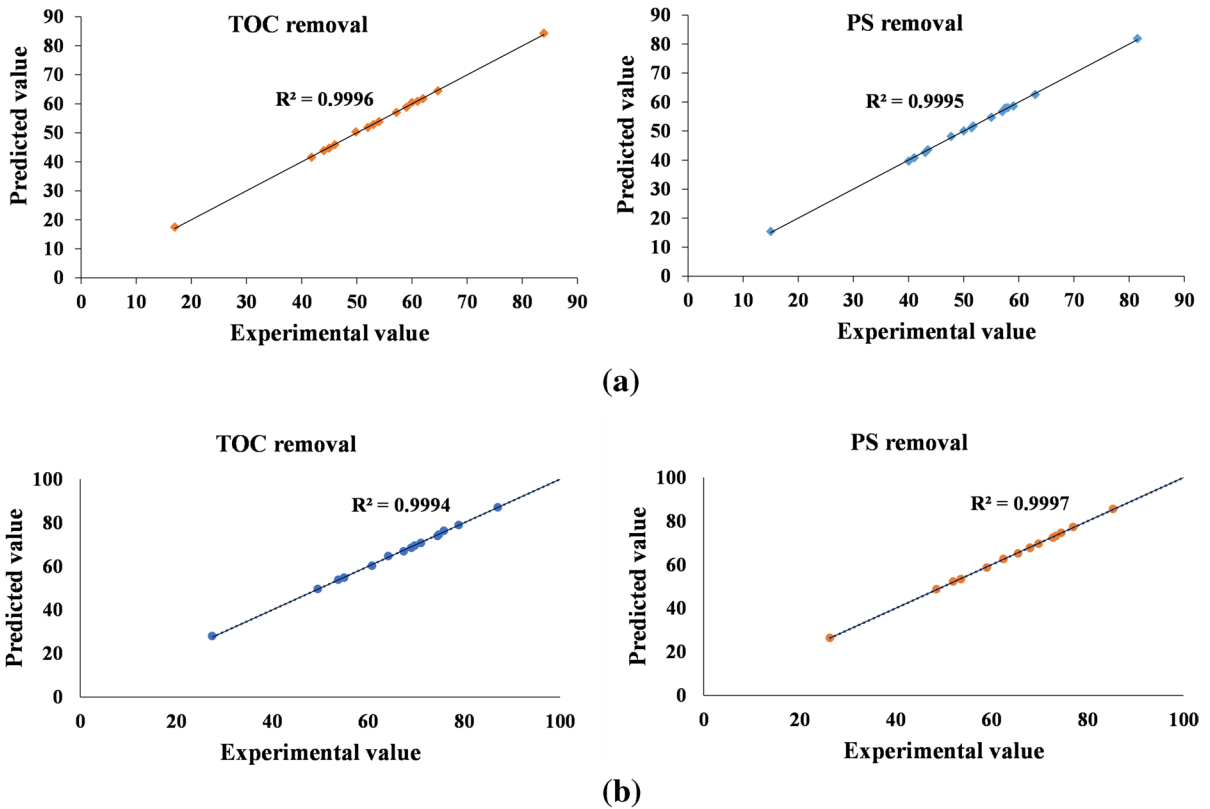


**Fig. 9** Experimental vs predicted values of TOC and PS removal in (a) EC process (b) EC- EO process

**Table 7** Optimum Conditions obtained by Taguchi  $L_{16}$  OA techniques for EC and EC-EO process

| Process | Response    | Operating condition   | Experiment value (%) | Predicted value (%) | Error (%) | CI (%)          | EEC (KWh/g pollutant remove) | OC (USD/m <sup>3</sup> ) |
|---------|-------------|---|----------------------|---------------------|-----------|-----------------|------------------------------|--------------------------|
| EC      | TOC removal | CD: 14.25 mA/cm <sup>2</sup> , pH <sub>i</sub> : 4, RSE: 70 rpm, PS <sub>i</sub> : 0.25 g/L | 83.93                | 84.36               | 0.43      | (82.56, 86.16)  | 0.135                        | 1.73                     |
|         | PS removal  | CD: 14.25 mA/cm <sup>2</sup> , pH <sub>i</sub> : 4, RSE: 70 rpm, PS <sub>i</sub> : 0.25 g/L | 81.19                | 81.96               | 0.77      | (79.90, 84.03)  | 0.056                        |                          |
| EC-EO   | TOC removal | CD: 14.25 mA/cm <sup>2</sup> , pH <sub>i</sub> : 4, RSE: 70 rpm, PS <sub>i</sub> : 0.25 g/L | 100                  | 100                 | 0         | (98.00, 103.09) | 0.113                        | 1.39                     |
|         | PS removal  | CD: 14.25 mA/cm <sup>2</sup> , pH <sub>i</sub> : 4, RSE: 70 rpm, PS <sub>i</sub> : 0.25 g/L | 100                  | 100                 | 0         | (98.49, 101.87) | 0.0453                       |                          |



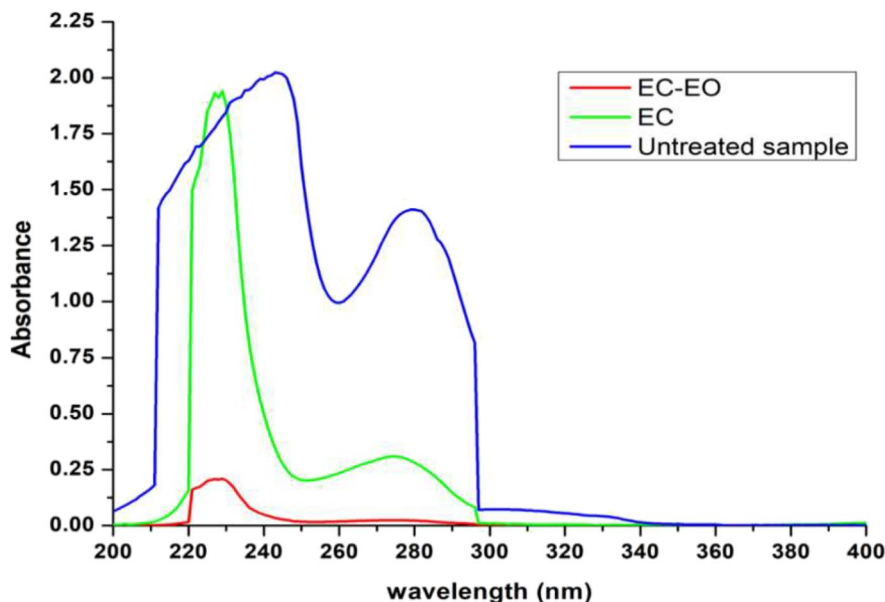
Vis spectroscopy, as this instrument is dependent on the interaction of electrochemical species with C=C or C=O and the degradation of the benzene ring, which reduces or removes the aromaticity of organic compounds. The UV–VIS spectrum of the PS solution has been recorded throughout a wavelength range of 200–400 nm during the EC and EC-EO procedures. The maximum peak observed near 280 nm (C=C bonded and aromatic organic compounds) may correspond to PS molecule  $n\text{-}\pi^*$  transitions. Figure 10 displays that the reduction in absorbance at 280 nm was greater in the EC-EO process compared to the EC process. The shifting of UV–VIS absorbance to 225 nm may be due to the formation of carboxyl group (i.e., formic acid) due to the degradation of PS in the both processes. The peak at 280 nm was found to disappear after 50 min of ET in the EC-EO process and the colour of the synthetic wastewater changed to dark brown. After some time, this colour eventually faded due to the formation of several intermediary compounds (i.e. Hydroquinone, carboxylic acid, etc.) (Muruganathan et al., 2005; Sundarapandiyani et al., 2014).

The treated samples were sent for FT-IR analysis to understand the degradation pathway of phenolic syntan. Figure 11 displays the FT-IR spectrum of the untreated and treated PS samples of EC and EC-EO practices. In the untreated sample, the bands visible in the range between 1443 and 1572 and 1173  $\text{cm}^{-1}$  correlate to C=C stretching and C-H bending, revealing

that the PS contains an aromatic ring. The benzene ring holding the functional groups of syntan corresponds to the peaks in the range of 895 and 620  $\text{cm}^{-1}$ , also indicating the C-S stretching. The sharp peak around 1037  $\text{cm}^{-1}$  is attributed to the S=O stretching vibrations of  $\text{SO}_3\text{H}$  bonded to the phenol ring.

Under the best working conditions, the FT-IR results of the EC and EC-EO treated samples revealed that the aromatic content and sulphonic group that are attached to the phenolic ring were entirely removed by the EC-EO process, unlike that in the EC process. The acute peak at instance magnitude of about 1640  $\text{cm}^{-1}$  in EC and EC-EO process treated samples had a characteristic  $\nu(\text{C}=\text{O})$  vibration associated with the quinone functional group. The new acute peak at an instance magnitude of about 1640  $\text{cm}^{-1}$  in the treated samples from EC and EC-EO process- had a characteristic  $\nu(\text{C}=\text{O})$  vibration associated with the quinone functional group. The new moderate intensity peak at 1399  $\text{cm}^{-1}$  in the EC-EO treated sample may be attributed to C-O-H bending. A new low-intensity peak at 1000  $\text{cm}^{-1}$  in the EC treated sample and a medium intensity peak at 1015.26  $\text{cm}^{-1}$  EC-EO treated sample could be attributed to the COOH bending vibrations. Thus, the FT-IR spectra indicated the presence of carboxylic acids in the treated samples of both the EC and EC-EO processes. The PS is expected to eventually get oxidized to  $\text{CO}_2$  and  $\text{H}_2\text{O}$  via low molecular weight carboxylic acids such as formic and oxalic acids.

**Fig. 10** UV–Vis spectrum for untreated sample, EC treated sample and EC-EO treated sample [CD = 14.25  $\text{mA}/\text{cm}^2$ ,  $\text{pH}_i = 4$ , RSE = 70 rpm,  $\text{PS}_i = 0.25 \text{ g/L}$ , electrolysis time = 50 min]



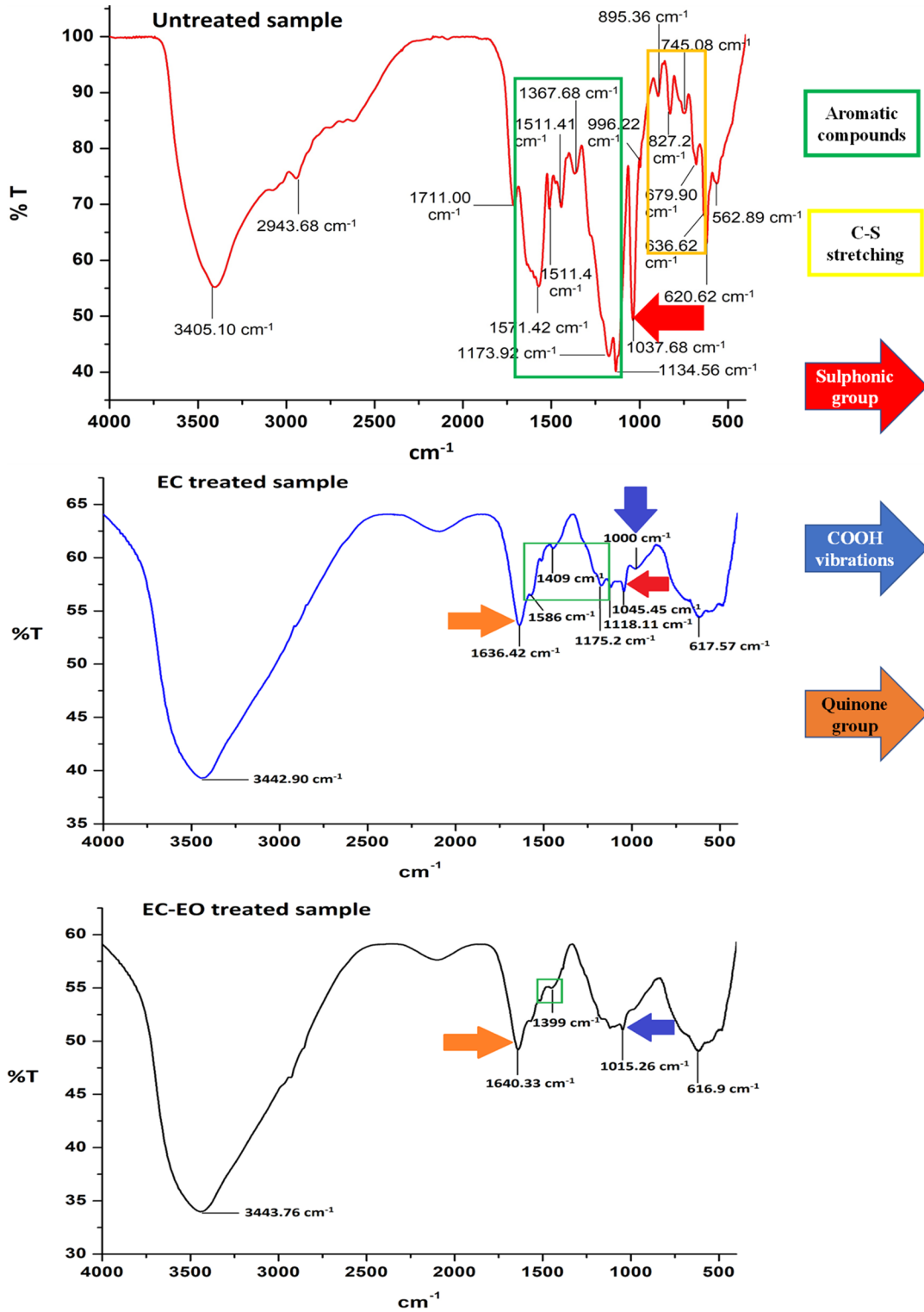


**Fig. 11** FT-IR spectrum for untreated sample, EC treated sample and EC-EO treated sample [CD=14.25 mA/cm<sup>2</sup>, pH<sub>i</sub>=4, RSE=70 rpm, PS<sub>i</sub>=0.25 g/L, electrolysis time=50 min]

## 4 Conclusions

A comparative study between the conventional EC and the combined EC-EO process was performed to evaluate the efficiency of PS removal from synthetic tannery wastewaters. The energy consumption and operating costs were also calculated for both the electrochemical processes. The EC process was operated with a rotating Al anode, whereas the EC-EO process had a rotating composite anode (Al-Ti/Pt-RuO<sub>2</sub>). The Taguchi L<sub>16</sub> method was used to optimize the operating conditions of the EC and EC-EO processes for maximum PS removal. This study demonstrated that the combined EC-EO process had higher PS removal efficiency, lower energy consumption and lower operating costs in comparison to the EC process. The major outcomes of this investigation are as follows:

1. OVAT results showed that the EC process required 90 min of ET for 80.7% of TOC removal and 79.43% of PS removal. Whereas, the EC-EO process required 20 min of ET for achieving the same removal efficiency at similar operating conditions (CD: 14.25 mA/cm<sup>2</sup>, pH<sub>i</sub>: 4, RSE: 70 rpm and PS<sub>i</sub>: 0.5 g/L). Therefore, the EC-EO process was found to consume less energy and had lower operating costs than the EC process.
2. At the optimum operating conditions obtained by the Taguchi L<sub>16</sub> method (CD: 14.25 mA/cm<sup>2</sup>, pH<sub>i</sub>: 4, RSE: 70 rpm and PS<sub>i</sub>: 0.25 g/L), the EC process achieved a TOC reduction of 84.36% and PS removal of 81.96%, with an operating cost of 1.73 USD/m<sup>3</sup>. However, complete mineralization of TOC and PS could be attained only by the combined EC-EO process with an operating cost of 1.39 USD/m<sup>3</sup>.
3. As per the S–N ratio and ANOVA analysis, CD was the most significant input operational factor for both processes. Whereas, RSE and pH<sub>i</sub> were the least effective parameters in the EC and EC-EO process, respectively.
4. UV/vis and FT-IR spectral analysis indicated that the EC-EO process achieved the maximum degradation of aromatic compounds compared to the EC process. Phenolic syntan was converted into the quinone functional group, which subsequently oxidized into low molecular weight carboxylic acids.

Based on the findings of the present study, the EC-EO procedure can be recommended as an effective alternative approach for the treatment of PS bearing tannery wastewaters. The optimum operating condition obtained by the Taguchi method can be used as a guideline for operating the EC-EO systems applied at large-scale up.

**Acknowledgements** The authors are grateful to the Department of Civil Engineering at MNNIT Allahabad for all their assistance in carrying out the research and to colleagues for providing valuable input and help at various stages of the investigation.

**Authors' contributions** Every author helped to discover concepts and design. AK was in charge of designing the experimental apparatus and material preparation. Under the guidance of DB, AK carried out experimentation and data analysis. AK wrote the initial draft of the manuscript, which was subsequently improved with the help of all of the authors.

**Funding** NA.

**Data Availability** The collection of data in a recent study are based on experiments performed by the author for his PhD program and can be shared on reasonable request with due permission of his thesis supervisor and the institute.

**Declarations**

**Ethics approval and consent to participate** Not applicable.

**Consent for publication** Not applicable.

**Conflict of Interest** The authors declare that they have no Conflict of Interest.

## References

- Aber, S., Amani-Ghadim, A. R., & Mirzajani, V. (2006). Removal of Cr(VI) from polluted solutions by electrocoagulation: Modeling of experimental results using artificial neural network. *Journal of Hazardous Materials*, 171, 484–490.
- Adhoum, N., & Monser, L. (2004). Decolourization and removal of phenolic compounds from olive mill wastewater by electrocoagulation. *Chemical Engineering and Processing: Process Intensification*, 43(10), 1281–1287. <https://doi.org/10.1016/j.cep.2003.12.001>
- Afroze, S., & Sen, T. K. (2018). A Review on Heavy Metal Ions and Dye Adsorption from Water by Agricultural Solid Waste Adsorbents. *Water, Air, & Soil Pollution*,

- 229(7). <https://doi.org/10.1007/s11270-018-3869-z> <https://doi.org/10.1007/s11270-018-3869-z>
- AlJaberi, F. Y. (2019). Modelling current efficiency and ohmic potential drop in an innovated electrocoagulation reactor. *Desalination and Water Treatment*, *164*, 102–110. <https://doi.org/10.5004/dwt.2019.24452>
- Anglada, A., Urriaga, A. M., & Ortiz, I. (2010). Laboratory and pilot plant scale study on the electrochemical oxidation of landfill leachate. *Journal of Hazardous Materials*, *181*(1–3), 729–735. <https://doi.org/10.1016/j.jhazmat.2010.05.073>
- Balki, M. K., Sayin, C., & Sarkaya, M. (2016). Optimization of the operating parameters based on Taguchi method in an SI engine used pure gasoline, ethanol and methanol. *Fuel*, *180*, 630–637. <https://doi.org/10.1016/j.fuel.2016.04.098>
- Belaid, C., Khadraoui, M., Mseddi, S., Kallel, M., Elleuch, B., & Fauvarque, J. F. (2013). Electrochemical treatment of olive mill wastewater: Treatment extent and effluent phenolic compounds monitoring using some uncommon analytical tools. *Journal of Environmental Sciences*, *25*(1), 220–230. [https://doi.org/10.1016/s1001-0742\(12\)60037-0](https://doi.org/10.1016/s1001-0742(12)60037-0)
- Benhadji, A., Ahmed, M. T., & Maachi, R. (2011). Electrocoagulation and effect of cathode materials on the removal of pollutants from tannery wastewater of Rouïba. *Desalination*, *277*, 128–134.
- Buso, A., Balbo, L., Giomo, M., Farnia, G., & Sandonà, G. (2000). Electrochemical Removal of Tannins from Aqueous Solutions. *Industrial & Engineering Chemistry Research*, *39*(2), 494–499. <https://doi.org/10.1021/ie990192a.59830>
- Can, O. T., Kobya, M., Demirbas, E., & Bayramoglu, M. (2006). Treatment of the textile wastewater by combined electrocoagulation. *Chemosphere*, *62*(2), 181–187.
- Cañizares, P., García-Gómez, J., Sáez, C., & Rodrigo, M. A. (2004). Electrochemical oxidation of several chlorophenols on diamond electrodes: Part II. Influence of waste characteristics and operating conditions. *Journal of Applied Electrochemistry*, *34*, 87–94. <https://doi.org/10.1023/B:JACH.0000005587.52946.66>
- Chen, G. (2004). Electrochemical technologies in wastewater treatment. *Separation and Purification Technology*, *38*, 11–41. <https://doi.org/10.1016/j.seppur.2003.10.006>
- Ciorba, G., Radovan, C., Vlaicu, I., & Masu, S. (2002). Removal of nonylphenol ethoxylates by electrochemically-generated coagulants. *Journal of Applied Electrochemistry*, *32*, 561–567. <https://doi.org/10.1023/A:1016577230769>
- Daghrir, R., Drogui, P., Blais, J. F., & Mercier, G. (2012). Hybrid Process Combining Electrocoagulation and Electro-Oxidation Processes for the Treatment of Restaurant Wastewaters. *Journal of Environmental Engineering*, *138*, 1146–1156.
- Daneshvar, N., Oladegaragoze, A., & Djafarzadeh, N. (2006). Decolorization of basic dye solutions by electrocoagulation: An investigation of the effect of operational parameters. *Journal of Hazardous Materials*, *129*(1–3), 116–122.
- Danhong, S., Qiuang, H., Wenjun, Z., Yulu, W., & Bi, S. (2008). Evaluation of environmental impact of typical leather chemicals. Part II, biodegradability of organic tanning agents by activated sludge. *Journal of the Society of Leather Technologists and Chemists*, *92*(2), 59–64.
- Dhawane, S. H., Kumar, T., & Halder, G. (2016). Biodiesel synthesis from Hevea brasiliensis oil employing carbon supported heterogeneous catalyst: Optimization by Taguchi method. *Renewable Energy*, *89*, 506–514.
- Dirany, A., Sirés, I., Oturan, N., Özcan, A., & Oturan, M. A. (2012). Electrochemical Treatment of the Antibiotic Sulfachloropyridazine: Kinetics, Reaction Pathways, and Toxicity Evolution. *Environmental Science & Technology*, *46*(7), 4074–4082. <https://doi.org/10.1021/es204621q>
- El-Ashtoukhy, E.-S.Z., Amin, N. K., & Abdelwahab, O. (2009). Treatment of paper mill effluents in a batch-stirred electrochemical tank reactor. *Chemical Engineering Journal*, *146*(2), 205–210. <https://doi.org/10.1016/j.cej.2008.05.037>
- Fajardo, A. S., Seca, H. F., Martins, R. C., Corceiro, V. N., Freitas, I. F., Quinta-Ferreira, M. E., & Quinta-Ferreira, R. M. (2017). Electrochemical oxidation of phenolic wastewaters using a batch-stirred reactor with NaCl electrolyte and Ti/RuO<sub>2</sub> anodes. *Journal of Electroanalytical Chemistry*, *785*, 180–189. <https://doi.org/10.1016/j.jelechem.2016.12.033>
- Feng, Y. J., & Li, X. Y. (2003). Electro-catalytic oxidation of phenol on several metal-oxide electrodes in aqueous solution. *Water Research*, *37*(10), 2399–2407. [https://doi.org/10.1016/s0043-1354\(03\)00026-5](https://doi.org/10.1016/s0043-1354(03)00026-5)
- Ferella, F., Michelis, L. D., Zerbini, C., & Veglio, F. (2013). Advanced treatment of industrial wastewater by membrane filtration and ozonisation. *Desalination*, *313*, 1–11.
- Fernandes, A., Santos, D., Pacheco, M. J., Ciriaco, L., & Lopes, A. (2016). Electrochemical oxidation of humic acid and sanitary landfill leachate: Influence of anode material, chloride concentration and current density. *Science of the Total Environment*, *541*, 282–291. <https://doi.org/10.1016/j.scitotenv.2015.09.052>
- Ganesh, R., & Ramanujam, R. A. (2009). Biological waste management of leather tannery effluents in India: Current options and future research needs. *International Journal of Environmental Engineering*, *1*, 165–186.
- Garcia, S. N., Clubbs, R. L., Stanley, J. K., Scheffe, B., Yelderman, J. C., & Brooks, B. W. (2013). Comparative analysis of effluent water quality from a municipal treatment plant and two on-site wastewater treatment systems. *Chemosphere*, *92*, 38–44. <https://doi.org/10.1016/j.chemosphere.2013.03.007>
- Garg, K. K., & Prasad, B. (2015). Removal of para-toluic acid (p-TA) from purified terephthalic acid (PTA) waste water by electrocoagulation process. *Journal of Environmental Chemical Engineering*, *3*(3), 1731–1739.
- Geng, R., Zhao, G. H., Liu, M. C., & Lei, Y. Z. (2010). *In situ* ESR Study of Hydroxyl Radical Generation on a Boron Doped Diamond Film Electrode Surface. *Acta Physico-Chimica Sinica*, *26*, 1493–1498.
- Ghalwa, N. A., Tamos, H., ElAskalni, M., & El Agha, A. R. (2012). Generation of sodium hypochlorite (NaOCl) from sodium chloride solution using C/PbO<sub>2</sub> and Pb/PbO<sub>2</sub>

- electrodes. *International Journal of Minerals, Metallurgy, and Materials*, 19(6), 561–566. <https://doi.org/10.1007/s12613-012-0596-0>
- Ginos, A., Manios, T., & Mantzavinos, D. (2006). Treatment of olive mill effluents by coagulation–flocculation hydrogen peroxide oxidation and effect on phytotoxicity. *Journal of Hazardous Materials*, 133, 135–142.
- Gokkus, O., Yıldız, Y. S., & Yavuz, B. (2012). Optimization of chemical coagulation of real textile wastewater using Taguchi experimental design method. *Desalination and Water Treatment*, 49, 263–271.
- Gonder, Z. B., Kaya, Y., Vergili, I., & Barlas, H. (2010). Optimization of filtration conditions for CIP wastewater treatment by nanofiltration process using Taguchi approach. *Separation and Purification Technology*, 70, 265–273. <https://doi.org/10.1016/j.seppur.2009.10.001>
- Gotsi, M., Kalogerakis, N., Psillakis, E., Samaras, P., & Mantzavinos, D. (2005). Electrochemical oxidation of olive oil mill wastewaters. *Water Research*, 39(17), 4177–4187. <https://doi.org/10.1016/j.watres.2005.07.037>
- Govindaraj, M., Muthukumar, M., & Bhaskar Raju, G. (2010). Electrochemical oxidation of tannic acid contaminated wastewater by RuO<sub>2</sub>/IrO<sub>2</sub>/TaO<sub>2</sub>-coated titanium and graphite anodes. *Environmental Technology*, 31(14), 1613–1622. <https://doi.org/10.1080/09593330.2010.482147>
- Gunes, S., Manay, E., Senyigit, E., & Ozceyhan, V. (2011). A Taguchi approach for optimization of design parameters in a tube with coiled wire inserts. *Applied Thermal Engineering*, 31, 2568–2577. <https://doi.org/10.1016/j.applthermaleng.2011.04.022>
- Guo, Z. R., Zhang, G., Fang, J., & Dou, X. (2006). Enhanced chromium recovery from tanning wastewater. *Journal of Cleaner Production*, 14(1), 75–79. <https://doi.org/10.1016/j.jclepro.2005.01.005>
- Gurses, A., Yalcin, M., & Dogar, C. (2022). Electrocoagulation of some reactive dyes: A statistical investigation of some electrochemical variables. *Waste Management*, 22, 491–499.
- Hassoune, J., Tahiri, S., Aarfane, A., El krati, M., Salhi, A., & Azzi, M. (2017). Removal of Hydrolyzable and Condensed Tannins from Aqueous Solutions by Electrocoagulation Process. *Journal of Environmental Engineering*, 143(6), 04017010. [https://doi.org/10.1061/\(asce\)je.1943-7870.0001196](https://doi.org/10.1061/(asce)je.1943-7870.0001196)
- Heidmann, I., & Calmano, V. (2008). Removal of Zn (II), Cu(II), Ni(II), Ag(I) and Cr (VI) present in aqueous solutions by aluminium electrocoagulation. *Journal of Hazardous Materials*, 152(3), 934–941.
- Hine, F. (1985). *Electrode Processes and Electrochemical Engineering*. Plenum Press.
- Holt, P. H., Barton, G. W., Wark, M., & Mitchell, A. A. (2002). A quantitative comparison between chemical dosing and electrocoagulation. *Colloids and Surfaces a: Physicochemical and Engineering Aspects*, 211, 233–248.
- Irdemez, S., Demircioglu, N., Yıldız, Y. S., & Bingul, Z. (2006). The effects of current density and phosphate concentration on phosphate removal from wastewater by electrocoagulation using aluminum and iron plate electrodes. *Separation and Purification Technology*, 52, 218–223. <https://doi.org/10.1016/j.seppur.2006.04.008>
- Jadhav, S. B., Chougule, A. S., Shah, D. P., Pereira, C. S., & Jadhav, J. P. (2014). Application of response surface methodology for the optimization of textile effluent biodecolorization and its toxicity perspectives using plant toxicity, plasmid nicking assays. *Clean Technologies and Environmental Policy*, 1–12. <https://doi.org/10.1007/s10098-014-0827-3>
- Jin, P., Chang, R., Liu, D., Zhao, K., Zhang, L., & Ouyang, Y. (2014). Phenol degradation in an electrochemical system with TiO<sub>2</sub>/activated carbon fiber as electrode. *Journal of Environmental Chemical Engineering*, 2(2), 1040–1047.
- Karthikeyan, S., Kumar, M. A., Maharaja, P., Partheeban, T., Sridevi, J., & Sekaran, G. (2014). Process optimization for the treatment of pharmaceutical wastewater catalyzed by poly sulphate sponge. *Journal of the Taiwan Institute of Chemical Engineers*, 45, 1739–1747. <https://doi.org/10.1016/j.jtice.2014.01.009>
- Khorshidi, B., Thundat, T., Fleck, B. A., & Sadrzadeh, M. (2015). Thin film composite polyamide membranes: Parametric study on the influence of synthesis conditions. *RSC Advance*, 5, 54985–54997. <https://doi.org/10.1039/C5RA08317F>
- Khosla, N. K., Venkatachalam, S., & Somasundaran, P. (1991). Pulsed electro- generation of bubbles for electroflotation. *Journal of Applied Electrochemistry*, 21, 986–990.
- Kim, T. H., Park, Ch., Shin, E. B., & Kim, S. (2002). Decolorization of disperse and reactive dyes by continuous electrocoagulation process. *Desalination*, 150, 165–175.
- Kobya, M., Can, O. T., & Bayramoglu, M. (2003). Treatment of textile wastewaters by electrocoagulation using iron and aluminum electrodes. *Journal of Hazardous Materials*, 100(1–3), 163–178.
- Kumar, A., & Basu, D. (2022a). Optimization of removal of Cr (VI) from wastewater by electrocoagulation process using Response Surface Methodology. *Journal of Hazardous, Toxic, and Radioactive Waste*. [https://doi.org/10.1061/\(ASCE\)HZ.2153-5515.0000723](https://doi.org/10.1061/(ASCE)HZ.2153-5515.0000723)
- Kumar, A., & Basu, D. (2022b). Economic and performance evaluation of electrocoagulation unit for the treatment of hexavalent chromium using Taguchi method. *International Journal of Environmental Science and Technology*. <https://doi.org/10.1007/s13762-022-04439-7>
- Kumar, A., & Basu, D. (2023). Parametric optimization of hexavalent chromium removal by electrocoagulation technology with vertical rotating cylindrical aluminum electrodes using Taguchi and ANN model. *Journal of Environmental Health Science and Engineering*, 21(1), 255–275.
- Li, M., Feng, C., Hu, W., Zhang, Z., & Sugiura, N. (2009). Electrochemical degradation of phenol using electrodes of Ti/RuO<sub>2</sub>-Pt and Ti/IrO<sub>2</sub>-Pt. *Journal of Hazardous Materials*, 162(1), 455–462. <https://doi.org/10.1016/j.jhazmat.2008.05.063>
- Li, H., Huang, G., An, C., Hu, J., & Yang, S. (2013). Removal of Tannin from Aqueous Solution by Adsorption onto Treated Coal Fly Ash: Kinetic, Equilibrium, and Thermodynamic Studies. *Industrial & Engineering Chemistry Research*, 52, 15923–15931.
- Li, P., Cai, W., Xiao, Y., Wang, Y., & Fan, J. (2017). Electrochemical degradation of phenol wastewater by SnSb-Ce modified granular activated carbon. *International Journal of Electrochemical Science*, 12, 2777–2790.

- Linares-Hernandez, I., Barrera-Díaz, C., Bilyeu, B., Juárez-GarcíaRojas, P., & Campos-Medina, E. (2010). A combined electrocoagulation-electrooxidation treatment for industrial wastewater. *Journal of Hazardous Materials*, *175*, 688–694. <https://doi.org/10.1016/j.jhazmat.2009.10.064>
- Lofrano, G., Meriç, S., Belgiorno, V., Nikolaou, A. N., Gallo, M., & Napoli, R. M. A. (2007). Fenton and Photo-Fenton treatment of a synthetic tannin used in leather tannery: A multi-approach study. *Water Science and Technology*, *55*(10), 53–61.
- Lofrano, G., Aydin, E., Russo, F., Guida, M., Belgiorno, V., & Meric, S. (2008). Characterization, fluxes and toxicity of leather tanning bath chemicals in a large tanning district area (IT). *Water Air Soil Pollution*, *8*, 529–542. <https://doi.org/10.1007/s11267-008-9177-7>
- Luu, T. L. (2020). Tannery wastewater treatment after activated sludge pre-treatment using electro-oxidation on inactive anodes. *Clean Technologies and Environmental Policy*. 2020. <https://doi.org/10.1007/s10098-020-01907-x>
- Mandal, P., Dubey, B. K., & Gupta, A. K. (2017). Review on landfill leachate treatment by electrochemical oxidation: Drawbacks, challenges and future scope. *Waste Management*, *69*, 250–273. <https://doi.org/10.1016/j.wasman.2017.08.034>
- Mansouri, K., Ibrik, K., Bensalah, N., & Abdel-Wahab, A. (2011). Anodic Dissolution of Pure Aluminum during Electrocoagulation Process: Influence of Supporting Electrolyte, Initial pH, and Current Density. *Industrial & Engineering Chemistry Research*, *50*(23), 13362–13372. <https://doi.org/10.1021/ie201206d10.1021/ie201206d>
- Michalowicz, J., & Duda, W. (2007). Phenols – Sources and Toxicity. *Polish Journal of Environmental Studies*, *16*(3), 347–362.
- Min, K. S., Yu, J. J., Kim, Y. J., & Yun, Z. (2004). Removal of Ammonium from Tannery Wastewater by Electrochemical Treatment. *Journal of Environmental Science and Health, Part A*, *39*(7), 1867–1879. <https://doi.org/10.1081/ese-120037884>
- Miriam, G., Rodriguez, R., Mendoza, V., Puebla, H., Sergio, A., & Martínez, D. (2019). Removal of Cr(VI) from wastewaters at semi-industrial electrochemical reactors with rotating ring electrodes. *Journal of Hazardous Materials*, *163*, 1221–1229.
- Moreira, F. C., Boaventura, R. A. R., Brillas, E., & Vilar, V. J. P. (2017). Electrochemical advanced oxidation processes: A review on their application to synthetic and real wastewaters. *Applied Catalysis b: Environmental*, *202*, 217–261. <https://doi.org/10.1016/j.apcatb.2016.08.037>
- Muruganathan, M., Bhaskar Raju, G., & Prabhakar, S. (2005). Removal of tannins and polyhydroxy phenols by electrochemical techniques. *Journal of Chemical Technology & Biotechnology*, *80*(10), 1188–1197. <https://doi.org/10.1002/jctb.1314>
- Nicolla, E. D., Meric, S., Gallo, M., Iaccarino, M., Rocca, C. D., Lofrano, G., Russo, T., & Pagano, G. (2007). Vegetable and synthetic tannins induce hormesis/toxicity in sea urchin early development and in algal growth. *Environmental Pollution*, *146*(1), 46–54.
- Olya, M. E., & Pirkarami, A. (2013). Electrocoagulation for the removal of phenol and aldehyde contaminants from resin effluent. *Water Science and Technology*, *68*(9), 1940–1949. <https://doi.org/10.2166/wst.2013.439>
- Ozgunay, H., Colak, S., Mutlu, M. M., & Akyuz, F. (2007). Characterization of leather industry wastes. *Polish Journal of Environmental Studies*, *16*, 867–873.
- Ozyonar, F., & Korkmaz, M. U. (2022). Sequential use of the electrocoagulation-electrooxidation processes for domestic wastewater treatment. *Chemosphere*, *290*, 133172. <https://doi.org/10.1016/j.chemosphere.2021.133172>
- Panizza, M. (2000). Electrochemical treatment of wastewater containing polyaromatic organic pollutants. *Water Research*, *34*(9), 2601–2605. [https://doi.org/10.1016/S0043-1354\(00\)00145-7](https://doi.org/10.1016/S0043-1354(00)00145-7)
- Panizza, M., & Cerisola, G. (2005). Application of diamond electrodes to electrochemical processes. *Electrochimica Acta*, *51*(2), 191–199. <https://doi.org/10.1016/j.electacta.2005.04.023>
- Radjenovic, J., & Sedlak, D. L. (2015). Challenges and opportunities for electrochemical processes as next-generation technologies for the treatment of contaminated water. *Environmental Science and Technology*, *49*, 11292–11302. <https://doi.org/10.1021/acs.est.5b02414>
- Rajkumar, D., Song, B. J., & Kim, J. G. (2007). Electrochemical degradation of reactive blue 19 in chloride medium for the treatment of textile dyeing wastewater with identification of intermediate compounds. *Dyes and Pigments*, *72*(1), 1–7.
- Raju, G. B., Karuppiah, M. T., Latha, S. S., Parvathy, S., & Prabhakar, S. (2008). Treatment of wastewater from synthetic textile industry by electrocoagulation–electrooxidation. *Chemical Engineering Journal*, *144*(1), 51–58. <https://doi.org/10.1016/j.cej.2008.01.008>
- Rema, T., Parivallal, B., & Ramanujam, R. A. (2010). Studies on degradation of syntan used in leather tanning process using ozone. *International Journal of Environmental Science and Development*, *1*(3), 264–267.
- Rivera-Utrilla, J., Sánchez-Polo, M., & Zaror, C. A. (2002). Degradation of Naphthalene sulfonic acid by oxidation with ozone in aqueous phase. *Physical Chemistry Chemical Physics*, *4*, 1129–1134.
- Sarkka, H., Bhatnagar, A., & Sillanpaa, M. (2015). Recent developments of electrooxidation in water treatment - a review. *Journal of Electroanalytical Chemistry*, *754*, 46–56.
- Song, Z. Y., Zhou, J. T., Wang, J., Yan, B., & Du, C. H. (2003). Decolorization of azo dyes by *Rhodobacter sphaeroides*. *Biotechnology Letters*, *25*, 1815–1818.
- Stone, R. A., & Veevers, A. (1994). The Taguchi influence on designed experiments. *Journal of Chemometrics*, *8*(2), 103–110.
- Sun, D., Hong, X., Wu, K., Hui, K. S., Du, Y., & Hui, K. N. (2020). Simultaneous removal of ammonia and phosphate by electro-oxidation and electrocoagulation using RuO<sub>2</sub>-IrO<sub>2</sub>/Ti and microscale zero-valent iron composite electrode. *Water Research*, *169*, 115239. <https://doi.org/10.1016/j.watres.2019.115239>
- Sundarapandiyan, S., Chandrasekar, R., Ramanaiah, B., Krishnan, S., & Saravanan, P. (2010). Electrochemical oxidation and reuse of tannery saline wastewater. *Journal of Hazardous Materials*, *180*(1–3), 197–203. <https://doi.org/10.1016/j.jhazmat.2010.04.013>

- Sundarapandiyan, S., Renitha, T. S., Sridevi, J., Chandrasekaran, B., Saravanan, P., & Raju, G. B. (2014). Mechanistic insight into active chlorine species mediated electrochemical degradation of recalcitrant phenolic polymers. *RSC Advances*, 4(104), 59821–59830. <https://doi.org/10.1039/c4ra09069a>
- Sundarapandiyan, S., Renitha, T. S., Sridevi, J., Saravanan, P., Chandrasekaran, B., & Raju, G. B. (2017). Photocatalytic degradation of highly refractive phenolic polymer – Mechanistic insights as revealed by Electron Spin Resonance (ESR) and solid-state  $^{13}\text{C}$  NMR spectroscopy. *Chemical Engineering Journal*, 313, 1112–1121. <https://doi.org/10.1016/j.cej.2016.11.009>
- Taguchi, G. (1990). *Introduction to Quality Engineering*. McGraw-Hill.
- Taguchi, G. (1986). *Introduction to quality engineering: designing quality into products and processes*. Asian Productivity Organization, Tokyo.
- Tavares, M. G., da Silva, L. V. A., Sales Solano, A. M., Tonholo, J., Martínez-Huitle, C. A., & Zanta, C. L. P. S. (2012). Electrochemical oxidation of Methyl Red using Ti/Ru0.3Ti0.7O2 and Ti/Pt anodes. *Chemical Engineering Journal*, 204–206, 141–150. <https://doi.org/10.1016/j.cej.2012.07.056>
- Thankappan, R., Srinivasan, S. V., Suthanthararajan, R., & Silanpää, M. (2017). Studies on removal of phenol sulfonic acid-syntan in aqueous medium using ozonation. *Environmental Technology*. <https://doi.org/10.1080/09593330.2017.1355936>
- Tisler, T., & Koncan, J. Z. (1997). Comparative assessment of toxicity of phenol, formaldehyde and industrial wastewater to aquatic organisms. *Water, Air & Soil Pollution*, 97, 315–322.
- Tripathi, M., Vikram, S., Jain, R. K., & Garg, S. K. (2011). Isolation and growth characteristics of chromium (VI) and pentachlorophenol tolerant bacterial isolate from treated tannery effluent for its possible use in simultaneous bioremediation. *Indian Journal of Microbiology*, 51(1), 61–69.
- Vijayalakshmi, P., Raju, G. B., & Gnanamani, A. (2011). Advanced Oxidation and Electrooxidation As Tertiary Treatment Techniques to Improve the Purity of Tannery Wastewater. *Industrial & Engineering Chemistry Research*, 50(17), 10194–10200.
- Virginija, J., Jiyembetova, I., Gulbinieniene, A., Sirvaityte, J., Beleska, K., & Urbelis, V. (2014). Comparable evaluation of leather waterproofing behaviour upon hide quality II. influence of retanning and fatliquoring agents on leather structure and properties. *Materials Science*, 20(2), 165–170.
- Voccianti, M., Menshova, I. I., & Ferro, S. (2021). Electrochemical Incineration of Synthetic Tannins Used in Retanning Processes. *Theoretical Foundations of Chemical Engineering*, 55(4), 618–627.
- Wu, Z., & Zhou, M. (2001). Partial Degradation of Phenol by Advanced Electrochemical Oxidation Process. *Environmental Science & Technology*, 35(13), 2698–2703. <https://doi.org/10.1021/es001652q10.1021/es001652q>
- Yoon, J. H., Yang, J., Shim, Y. B., & Won, M. S. (2007). Electrochemical degradation of benzoquinone in a flow through cell with carbon fiber. *Bulletin of the Korean Chemical Society*, 28, 403–407.
- Zhu, X., Ni, J., Wei, J., Xing, X., Li, H., & Jiang, Y. (2010). Scale-up of BDD anode system for electrochemical oxidation of phenol simulated wastewater in continuous mode. *Journal of Hazardous Materials*, 184, 493–498. <https://doi.org/10.1016/j.jhazmat.2010.08.062>
- Zolgharnein, J., Asanjrani, N., & Shariatmanesh, T. (2013). Taguchi  $L_{16}$  orthogonal array optimization for cd(II) removal using *Carpinus betulus* tree leaves: Adsorption characterization. *International Biodeterioration & Biodegradation*, 85, 66–77.
- Zolgharnein, J., Asanjrani, N., Bagtash, M., & Azimi, G. (2014). Multi-response optimization using Taguchi design and principle component analysis for removing binary mixture of alizarin red and alizarin yellow from aqueous solution by nano  $\gamma$ -alumina. *Spectrochimica Acta Part a: Molecular and Biomolecular Spectroscopy*, 126, 291–300.

**Publisher's Note** Springer Nature remains neutral with regard to jurisdictional claims in published maps and institutional affiliations.

Springer Nature or its licensor (e.g. a society or other partner) holds exclusive rights to this article under a publishing agreement with the author(s) or other rightsholder(s); author self-archiving of the accepted manuscript version of this article is solely governed by the terms of such publishing agreement and applicable law.